Evaluation of flow resistance in gravel-bed rivers through a large field data set

Dieter Rickenmann[1] and Alain Recking[2]

Received 23 July 2010; revised 15 April 2011; accepted 27 April 2011; published 21 July 2011.

[1] A data set of 2890 field measurements was used to test the ability of several conventional flow resistance equations to predict mean flow velocity in gravel bed rivers when used with no calibration. The tests were performed using both flow depth and discharge as input since discharge may be a more reliable measure of flow conditions in shallow flows. Generally better predictions are obtained when using flow discharge as input. The results indicate that the Manning-Strickler and the Keulegan equations show considerable disagreement with observed flow velocities for flow depths smaller than 10 times the characteristic grain diameter. Most equations show some systematic deviation for small relative flow depth. The use of new definitions for dimensionless variables in terms of nondimensional hydraulic geometry equations allows the development of a new flow resistance equation. The best overall performance is obtained by the Ferguson approach, which combines two power law flow resistance equations that are different for deep and shallow flows. To use this approach with flow discharge as input, a logarithmic matching equation in terms of the new dimensionless variables is proposed. For the domains of intermediate and large-scale roughness, the field data indicate a considerable increase in flow resistance as compared with the domain of small-scale roughness. The Ferguson approach is used to discuss the importance of flow resistance partitioning for bed load transport calculations at flow conditions with intermediate- and large-scale roughness in natural gravel, cobble, and boulder bed streams.

Citation: Rickenmann, D., and A. Recking (2011), Evaluation of flow resistance in gravel-bed rivers through a large field data set, *Water Resour. Res., 47*, W07538, doi:10.1029/2010WR009793.

1. Introduction

[2] Knowledge of the mean flow velocity in a channel reach is of primary importance for many aspects, including river engineering, risk analysis, environmental survey, numerical modeling validation, flow discharge, and bed load transport computation. In some circumstances, flow velocity can be measured directly (for instance with a current meter) or be calculated with the continuity equation ($U = Q/A$) when both the discharge Q and the wetted cross-sectional area A are known. But in many cases measurements are not possible, and a flow resistance equation must be used. When a rating curve is available, the flow resistance equation can be fitted for the site in question. Several flow resistance equations are of interest because they need no calibration when the river reach can be considered nearly uniform. This paper proposes to use a large field data set in order to test the adequacy of these equations for predicting the mean flow velocity in a uniform gravel bed river reach.

[3] The Chezy, the Manning, and the Darcy-Weisbach equations are the most commonly used equations and are given by

$$U = C\sqrt{dS} = \frac{S^{1/2}d^{2/3}}{n} = \sqrt{\frac{8gdS}{f}}, \tag{1}$$

respectively, where U is the mean flow velocity, C ($L^{1/2}$ s^{-1}) is the Chezy coefficient, n ($L^{-1/3}s$) is the Manning coefficient, f (dimensionless) is the Darcy-Weisbach friction factor, S is the energy slope, d is the flow depth, and g is the acceleration of gravity. The hydraulic radius R is usually used instead of d for narrow channels. For deriving a general equation, many studies [e.g., *Strickler*, 1923; *Limerinos*, 1970; *Griffiths*, 1981] have tried to link these coefficients to bed and flow characteristics (flow discharge or depth, river width and slope, bed roughness). Because f is a nondimensional coefficient, most equations were derived for f. In a pioneering work, *Keulegan* [1938] integrated the Prandtl-Karman-Nikuradse logarithmic mean flow velocity profile equation to derive a logarithmic equation of the form

$$\sqrt{\frac{8}{f}} = \frac{U}{u^*} = 6.25 + \frac{1}{\kappa}\ln\left(\frac{d}{k_s}\right), \tag{2}$$

[1]Swiss Federal Research Institute WSL, Birmensdorf, Switzerland.
[2]UR Erosion Torrentielle Neige Avalanches, Cemagref, Saint-Martin-d'Hères, France.

0043-1397/11/2010WR009793

where $u^* = (gdS)^{0.5}$ is the shear velocity, κ is the Von Karman coefficient (0.4), and k_s is the bed roughness. Keulegan proposed using the median diameter D_{50} for k_s, but several expressions were given since that time in the form $k_s = cD_x$ (where $1 < c < 8$ and where the subscript x denotes percent finer than D). A comprehensive review of flow resistance equations was given by *Yen* [2002]. The Darcy-Weisbach equation was also expressed with a power function of the relative flow depth d/D [*Bray*, 1979; *Ferguson*, 2007] or even more complex exponential forms [*Smart and Jäggi*, 1983].

[4] However, for field studies, the flow discharge measurement in small and rough streams is usually much more accurate than the flow depth measurement. In these streams the often irregular bed topography and the water surface complicate the determination of a representative flow depth. This is why several authors proposed nondimensional hydraulic geometry equations that link the mean flow velocity to the flow discharge [*Rickenmann*, 1990, 1994, 1996; *Aberle and Smart*, 2003; *Comiti et al.*, 2007; *Ferguson*, 2007; *Zimmermann*, 2010]. These equations were generally given in a dimensionless form (equation (3)) and proved to perform better than other equations [*Ferguson*, 2007]:

$$U^* = kq^{*m}S^{(1-m)/2}, \tag{3}$$

where k and m are determined empirically, $U^* = U/(gD_{84})^{0.5}$, $q^* = q/(gD_{84}{}^3)^{0.5}$, and D_{84} is used as a characteristic grain size by Ferguson. He provided a detailed review of flow resistance equations in steep streams, and he showed that for shallow flows, equation (3) is consistent with a power function of d/D:

$$\sqrt{\frac{8}{f}} = a\left(\frac{d}{D_{84}}\right)^b. \tag{4}$$

[5] He also pointed out the equivalence between (3) and (4), implying the following relations: $k = a^{(1-m)}$, $m = (2b + 1)/(2b + 3)$, and $b = (3m - 1)/(2 - 2m)$. Field measurements for bed slopes up to $S = 0.184$ (resulting in $b = 1.80$, which is equivalent to $m = 0.7$) indicate that b and m should increase with S [*Lee and Ferguson*, 2002; *Comiti et al.*, 2007; *David et al.*, 2010b]. Furthermore, *Aberle and Smart* [2003] concluded that m should increase with bed slope on the basis of flume experiments. Similarly, *Bathurst* [2002] showed b (and thus m) to be larger for the investigated sites with $0.008 < S \leq 0.042$ than for sites with $S < 0.008$, and he suggested that b may decrease with increasing uniformity of the bed material distribution (which may be partly correlated with decreasing bed slope and increasing relative flow depth).

[6] Whatever approach was used, flow resistance equations proved to be more reliable for flow conditions for which the flow depth or the hydraulic radius is large compared to the bed roughness. *Bathurst et al.* [1981] proposed to classify flows according to the relative flow depth and defined a large-scale roughness ($d/D_{84} \leq 1.2$, the roughness features affect the free surface), an intermediate-scale roughness ($1.2 < d/D_{84} \leq 4$), and a small-scale roughness ($d/D_{84} > 4$, the flow can be described by the boundary layer theory). Modeling flow resistance for the large- and intermediate-scale roughness is still very challenging because the flow turbulence is strongly affected by relatively large bed elements in such flows. For these conditions, conventional equations such as equation (2) derived from the law of the wall may not be valid any longer. This is particularly true for steep mountain streams with step-pool morphology. On the basis of the idea of spatially averaging the flow over a rough bed, a similar distinction was proposed between flows with high relative flow depth, flows with small relative flow depth, and flows over a partially inundated rough bed [*Nikora et al.*, 2001, 2004].

[7] In this paper a large data set consisting of 2890 measurements is used to (1) evaluate the performance of several flow resistance equations, (2) demonstrate that simple equations perform as well as more complex approaches, and (3) discuss the importance of a strong increase in flow resistance for relative flow depths smaller than about 7. First, the data set is presented. Second, it is used to test the suitability of several conventional flow resistance equations. Third, new definitions for the dimensionless variables in terms of hydraulic regime equations are used to develop a new approach and as a basis to discuss flow resistance for very low relative depths and at-a-site variation of flow resistance. Finally, a flow resistance partitioning into "base level" resistance and "macroroughness" resistance is proposed for gravel, cobble, and boulder bed streams, which appears to improve bed load transport calculations for flow conditions with intermediate- and large-scale roughness.

2. The Data Set and Equations

[8] The initial data set used in this study is composed of 3942 measurements presented in Table 1 and Figure 1. The data represent field measurements of flow velocity in gravel bed streams, including channel slopes up to 24% and different channel bed morphologies. Parts of these data have already been used by *Recking et al.* [2008] and *Recking* [2010]. Other data are taken form *Church and Rood* [1983], and data from *Higginson and Johnston* [1988] are used as reported by *Wargadalam* [1993]. In these studies, flow velocity was obtained by several techniques, including the continuity from known flow discharge and cross-sectional area ($U = Q/A$) and direct measurements with either a current meter or a tracer injection. If the grain size D_{84} was missing, it was estimated by $2.2D_{50}$. This approximation is based on the median value for 141 pairs of available D_{50} and D_{84} values and concerns about 21% of the data used in the analysis. If the grain size D_{90} was missing, it was estimated by $1.25D_{84}$, with the approximation being based on the median value for 30 pairs of available D_{84} and D_{90} values and concerning about 78% of the data used in the analysis. Some data may not be of good quality because of either measurement errors or data set manipulation. Because a close inspection of all runs was not feasible, a first rough selection with the following criteria was made to remove so-called outliers: no friction values $(8/f)^{0.5}$ are allowed to be 30% higher than values predicted with the Keulegan law, which has been derived for flat bed, fine sands, and mild bed slopes and should consequently correspond to an upper limit for U/u^*. Similarly, no values are allowed to be 30% lower than values predicted by the

Table 1. Data Range and Sources of Field Data on Flow Resistance Measurements[a]

Reference	W (m)	Slope (%)	Q (m^3/s)	H (m)	U (m/s)	D_{50} (mm)	D_{84} (mm)	Measurement	Comment	N
Church and Rood [1983]	1–3100	0.004–8.01	0.06–16,950	0.04–13.9	0.09–4.7	0.15–268	NA	Several methods.	Data set compiled from 25 papers and reports written by different investigators. Essentially sinuous and meandering channels.	497
Hey and Thorne [1986]	5.5–77.1	0.12–2.15	0.1–424	0.1–3.21	0.9–3	14–176	NA	Q measured at gauging stations having at least 10 years of records, $U = Q/A$. Bankfull velocity.	62 locations. Riffle pools; self-formed channel in erodible material and free from constraints. Various degrees of bank vegetation cover.	62
Griffiths [1981]	2.9–153	0.009–1.1	0.05–2409	0.12–7.51	0.09–4.31	12–301	NA	Current meter.	72 reaches of 46 New Zealand rivers. Straight channels, little vegetation, wide trapezoidal channels.	136
Higginson and Johnston [1988]	2.8–2775	0.031–2.93	0.68–6754	0.55–176	0.28–161	0.12–400	NA	Bankfull conditions. Data were as reported by *Wargadalam* [1993]. No information about the velocity measurement technique.		68
Colosimo et al. [1988]	3–23	0.26–1.9	0.4–133	0.26–53	0.43–2.71	20.5–60	NA	Current meter.	43 reaches with quasi-uniform flow conditions and free from obstacles. Differences between discharges measured in the same reach not exceeding 10%.	43
Reid et al. [1995]	3.5	0.7–1	0.3–5	0.11–0.6	0.78–2.38	6	13	Deduced from surface velocity.	Straight channel in an ephemeral stream. Vegetated banks (xerophytes).	74
Andrews [1994]	2.57	0.95–1.1	1–3.12	0.35–1.6	1.1–1.96	58	104	Detailed vertical and cross-channel velocity profiles.	USGS gauging station operated since 1953. Bankfull discharge varied within 10%.	55
Leopold and Emmett [1976, 1977, 1997]	14.6	0.07	2–41.5	0.24–2.01	0.49–1.41	1.3	13	Stage discharge relation.	3.3 km long river reach meandering within a 120 m large flood plain.	184
Gomez [1988]	0.3–2.2	3	0.015–0.25	0.092–0.127	0.13–1.03		19	Flow depth and velocity (current meter).	Plane bed in a stable and well-defined river section, downstream a steep boulder section. A scour pool and a small longitudinal bar.	31
Ryan et al. [2002]	1.68–10.3	0.5–6.1	0.04–7.15	0.07–0.62	0.15–1.8		100–543	U measured with current meter. Q calculated with measured U and A.	Steep gravel, cobble, and boulder bed mountain streams. Stable and strongly armored beds. Stable banks with dense to moderately dense vegetative cover. Eight sites including three step pools and five pool-riffle–plane bed channels.	1009
Williams and Rosgen [1989]	1–469	0.011–8.56	0.023–7104	0.086–77	0.047–3.1		0.9–460	U measured by one of three methods: (1) standard streamflow gauging measurement, (2) rating curve hydraulic geometry $U(Q)$, or (3) $U = Q/A$ with Q and A measured.	Compilation of several field investigations. Data collected in 93 streams.	526
Samide [1971]	3–6.1	0.158–0.745	4.71–39.2	0.65–2.8	1.78–3.63			Direct flow velocity and depth measurement and $Q = UA$.	In the work of *Brownlie* [1981].	55
Bathurst [1985]	5.1–49.8	0.16–3.73	0.137–195	0.1–2.8	0.17–3.72		27.2–740	Q obtained at gauging stations close to the study sites. Cross-section survey.	Straight channels either on riffles between pools or over plane beds without pools.	44

Table 1. (continued)

Reference	W (m)	Slope (%)	Q (m^3/s)	H (m)	U (m/s)	D_{50} (mm)	D_{84} (mm)	Measurement	Comment	N
Jarrett [1984]	6.7–51.8	0.2–3.4	0.34–128.2	0.15–2.0	0.27–2.63		33.5–792	U measured with a current meter and concurrent water surface elevation.	Straight and uniform channel reaches with minimal vegetation	75
Thorne and Zevenbergen [1985]	10.3–18.9	1.43–1.98	2.05–10.45	0.3–0.64	0.52–1.42		337–393	Q obtained at gauging station with a precision of ±10%. Cross-section survey.	Two uniform reaches in a boulder mountain stream.	12
Wohl and Wilcox [2005]	2.2–38	0.3–24	1.3–194	0.2–1.9	1–3.6		140–1350	Salt tracer, bankfull discharge.	Step pool.	34
Bathurst [1978]	14.6–32.9	0.8–1.74	0.9–7.2	0.17–0.41	0.24–0.9		280–485	Q obtained at gauging stations close to the study sites. Cross-section survey.	Three straight and uniform boulder reaches, 100 m long, free of pools.	9
Orlandini et al. [2006]	1.5–8.8	2.8–18.1	0.017–0.775	0.17–0.37	0.067–0.51		249–963	Q measured at gauging station.	Step pool.	12
Barnes [1967]	7.7–130	0.084–3.2	3.91–1950	0.4–5	1.27–3		157–650	Current meter or stage-discharge relationship. Flows below bankfull in a uniform straight channel.	72 reaches of gravel, cobble, and boulder, vegetated and nonvegetated streams.	14
Coon [1998]	9–131	0.03–1.3	2.2–1464	0.4–5.1	0.3–4.3	15–366	43–914	Stage-discharge relations at USGS gauging stations (accuracy within 10%).	21 vegetated streams in New York state.	235
Reid and Hickin [2008]	1.7–20.45	1.7–70.5	0.03–5.52	0.06–0.54	0.03–1.07	105–190	200–570	Q measured with a current meter and cross-section survey.	13 reaches including pool riffles, plane bed, step pool, cascades, embanked vegetation, and woody debris.	616
David et al. [2010a]	0.67–4.04	1.7–19.5	0.01–1.85	0.19–1.03	0.11–1.67	10–80	50–170	U measured with the dye tracer technique. Cross-section survey with a laser theodolite.	15 channels reaches including step pools and cascades; woody debris and embanked vegetation.	59
Lepp et al. [1993]	0.65–2.13	11.2–14.6	0.01–0.47	0.04–0.25	0.1–1.04	84–114	220–298	U measured with brine solution (tracer technique). Survey of six cross sections in study reach.	3 reaches with channel bed consisting of gravel, cobbles, and scattered boulders.	72
Adenlof and Wohl [1994]	2.1–5.4	5.8–19.7	0.52–0.98	0.19–0.35	0.55–1.07	21–46	56–121	U measured with current meter at 0.6 of flow depth, Q obtained with survey of cross section area.	12 cross sections along 1 km reach, bed morphology includes step-pool structures and woody debris.	12
Lenzi [2001]	3.67–5.42	11–14	1–4.73	0.15–0.53	1.23–2.5	404–419	1060–1100	U measured with current meter, 2–3 points in 4–5 verticals and with crest stage gauges and Q at permanent gauging station for October 1998 peak flow.	2 step-pool reaches, about 30 and 60 m long.	8
All data	0.3–2775	0.004–24	0.01–16,950	0.04–176	0.03–161	0.12–650	0.31–1350			3942

[a]N, number of measurements; NA, not applicable.

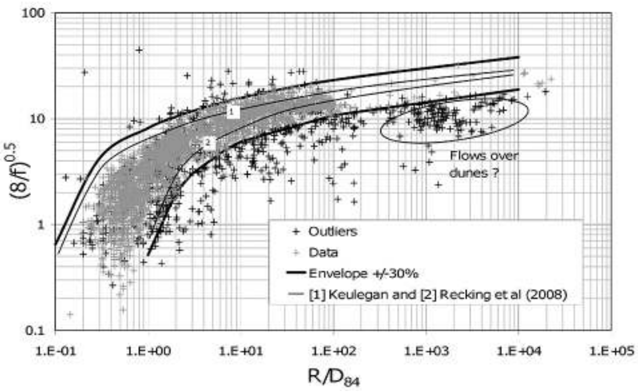

Figure 1. The field measurements shown in terms of $(8/f)^{0.5}$ versus R/D_{84}, distinguished between retained data (gray crosses) and excluded (black crosses) data. Because of the data selection procedure (see section 2) some excluded data are within the envelope ±30%.

friction law proposed by *Recking et al.* [2008] for very steep slopes and high sediment transport (including sheet flow regimes). For the purpose of developing a new approach, the field data were further examined regarding consistency of the continuity equation and a rectangular cross section for the determination of the hydraulic radius R. If $q = Ud$ differed by more than 5% from $q' = Q/W$ and if R given in the source document differed by more than 5% from $R' = Wd/(W + 2d)$, i.e., the hydraulic radius for a rectangular cross section, the data were excluded from further analysis. Here Q is total discharge, and W is channel width. The limiting discrepancy of 5% was selected because it can result from rounding errors associated with published values having only two digits. The selection of data satisfying the criterion $0.95 < R/R' < 1.05$ is made to facilitate comparison of flow resistance equations using either flow depth or discharge as input. Thus, the final data set consists of 2980 measurements and covers a large range of bed slopes, grain sizes, discharges, river widths, depths, and morphologies (pool riffles to cascades following *Montgomery and Buffington* [1997]). The data are plotted in Figure 1, with a distinction between retained and excluded values.

[9] For the performance evaluation, six equations were considered because they are widely used or because they represent a low or high degree of complexity:
Manning-Strickler [*Strickler*, 1923]

$$\sqrt{\frac{8}{f}} = 8.3\left(\frac{d}{D_{90}}\right)^{1/6}, \tag{5}$$

Keulegan [1938]

$$\sqrt{\frac{8}{f}} = 6.25 + 5.75\log\left(\frac{d}{D_{50}}\right), \tag{6}$$

Hey [1979]

$$\sqrt{\frac{8}{f}} = 6.25 + 5.75\log\left(\frac{d}{3.5D_{84}}\right), \tag{7}$$

Bathurst [1985]

$$\sqrt{\frac{8}{f}} = 4 + 5.62\log\left(\frac{d}{D_{84}}\right), \tag{8}$$

Smart and Jäggi [1983]

$$\sqrt{\frac{8}{f}} = 5.75\left[1 - \exp(-0.05Z_{90}/S_0^{0.5})\right]^{0.5}\log\left(8.2\frac{d}{D_{90}}\right), \tag{9}$$

Ferguson [2007]

$$\sqrt{\frac{8}{f}} = \frac{a_1\, a_2\, (d/D_{84})}{\sqrt{a_1^2 + a_2^2 (d/D_{84})^{5/3}}}, \tag{10a}$$

$$a_1^2\, U^{**^5} + a_2^2\, U^{**^{10/3}}\, q^{**^{5/3}} = a_1^2\, a_2^2\, q^{**^3}. \tag{10b}$$

The Manning-Strickler equation (5) is used with $n = D_{90^{1/6}}/26$. Equation (10b) results from a transformation of (10a) using the dimensionless variables introduced in section 3.2. Equations (10a) and (10b) are applied here with $a_1 = 6.5$ and $a_2 = 2.5$ as suggested by Ferguson (personal communication, 2010). The Keulegan equation [*Keulegan*, 1938] and the Smart and Jäggi equation [*Smart and Jäggi*, 1983] were derived from flume measurements, whereas the Manning-Strickler equation [*Strickler*, 1923], the Hey equation [*Hey*, 1979], the Bathurst equation [*Bathurst*, 1985], and the Ferguson equation [*Ferguson*, 2007] are mainly based on field measurements. These equations are plotted for comparison in Figure 2. All equations plot between *Keulegan* [1938] and *Hey* [1979], and the trend for all equations is very similar, except for low relative depths ($R/D < 10$). The envelope shown in Figure 1 permits a first estimation of the precision that can be expected in flow velocity prediction; for $R/D > 10$, the Keulegan equation predicts velocities 30% higher than the Hey equation. This ratio increases for low relative depth, reaching 100% for $R/D = 1$.

3. Comparison of Flow Resistance Equations

3.1. Evaluation of Existing Approaches

[10] The tests were performed using both flow depth and discharge as input. Discharge may be a more reliable measure of flow conditions in shallow flows, and discharge-based equations for velocity predictions in shallow flows were found to perform better than flow depth–based equations [*Ferguson*, 2007]. All equations are first tested with the hydraulic radius R (determined from the measured flow depth d). For comparison with measured velocities a simple discrepancy ratio A_r is used, defined as $A_r = U_{\text{calculated}}/U_{\text{measured}}$. The results are shown in Figure 3 as box plots in terms of R/D classes. The scores (percent of predictions within a given class of A_r values) are listed in Table 2a. The Manning-Strickler and the Keulegan equations clearly and systematically overestimate observed flow velocities

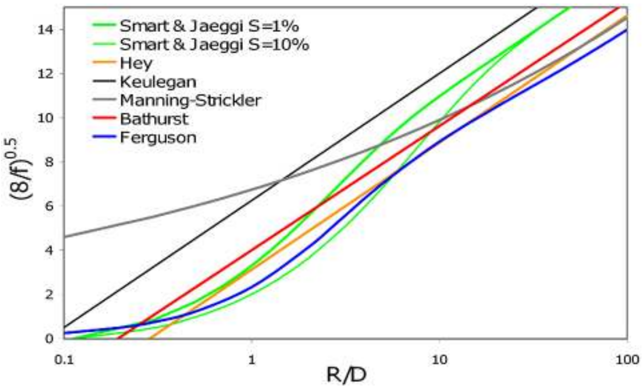

Figure 2. Graphical comparison of several flow resistance equations in terms of $(8/f)^{0.5}$ versus relative flow depth R/D.

for large- and intermediate-scale roughness (for R/D_{84} values smaller than about 7–10) and also have the lowest scores. For the following discussion, therefore, only the other equations are considered in more detail. The Bathurst equation results in an overestimation for very shallow flows with R/D_{84} values smaller than about 1, and for the range $0.5 < A_r < 1.5$ and R/D_{84} values smaller than about 10, the scores are not among the best performing equations (Table 2a). The other equations (Hey, Smart-Jäggi, and Ferguson) have the best overall performance. However, the apparent good performance of the Hey equation for the smallest class with $R/D_{84} < 0.7$ is degraded by the fact there are 30 predictions of negative flow velocities. This reflects an inherent problem of a log law approach for very small flow depth (a few negative flow velocities are also predicted by the Bathurst equation). Table 2b shows the presence or absence of systematic trends of the A_r values with one of the following variables: S, D_{84}, d/D_{84}, W, and q^{**}. The dimensionless variable q^{**} represents a dimensionless unit discharge, and its definition is introduced as equation (11) in section 3.2. Table 2b indicates that the variable power equation (VPE) of *Ferguson* [2007] has the best overall performance, showing the least tendency of a systematic trend for overprediction or underprediction as a function of the tested variables. The VPE approach combines two power law flow resistance equations that are different for deep and shallow flows.

[11] A second comparison is performed with the same equations but using Q or q as an input parameter. As a first step the method replaces U by $Q(W - 2R)/(RW^2)$ in the flow resistance equations, assuming a rectangular section, and determines R with an iterative calculation. In a second step, U is obtained by using the iteratively computed R value in the flow resistance equation. The implicit equation (10b) of the Ferguson approach is also solved iteratively for each given q^{**} value. Results presented in Table 3a show that the score obtained by each equation is greatly improved. The best scores are obtained by the Hey, Ferguson, and Smart-Jäggi (and partly Bathurst) equations. The results are shown in Figure 4 as box plots in terms of q^{**} classes. In Figure 4 discrepancy ratios A_r are shown for q^{**} classes with limits corresponding to the limits (R/D_{84}) in Figure 3, where q^{**} is determined from d/D_{84} instead of R/D_{84} (using equation (22)). The scores (percent of predictions within a given class of A_r values) are listed in Table 3a. Table 3b shows the presence or absence of systematic trends of the A_r values with one of the same variables as used in Table 2b. The generally better performance of the Q-based iteration or q^{**}-based procedure (as compared with the d-based predictions) is to be expected for the cases where the determination of q (and subsequently $Q = qW$) is based on the measured flow velocity U, i.e., where the determination of Q is not based on an independent measurement such as tracer dilution or a gauging station. The Manning-Strickler and the Keulegan equations show systematic underestimation and overestimation of observed flow velocities with changing (R/D_{84}), and they have the comparatively lowest scores. The other equations (Hey, Bathurst, Smart-Jäggi, and Ferguson) have a better overall performance. On the basis of Figure 4 and Tables 3a and 3b the best overall performance is obtained by the VPE of Ferguson, showing again the least tendency of a systematic trend for overprediction or underprediction as a function of the tested variables. For the discharge-based calculations, no negative velocity predictions with the log law approaches can occur.

3.2. Proposal of New Dimensionless Variables

[12] Despite the good overall performance of the best performing flow resistance equations (Hey equation (7), Smart-Jäggi equation (9), and Ferguson equations (10a) and (10b); Figures 3 and 4 and Tables 2a, 2b, 3a, and 3b), there are some limitations: the log law equations can have problems at very small relative flow depths if applied in terms of d. For situations for which the discharge is known or given, the use of a traditional log law equation or of the VPE approach of Ferguson requires a partly complicated iterative solution procedure. This represents a practical disadvantage, for example, in catchment-based studies when a hydrograph is available from hydrologic considerations or for design problems in river engineering. In addition, some limitations are apparent for most equations if applied in the range of intermediate- and large-scale roughness ($d/D_{84} <$ 4). Given these limitations, an alternative approach is developed on the basis of new dimensionless variables. These variables are used in section 5 to consider flow resistance for very low relative flow depths and to discuss at-a-site variation of flow resistance.

[13] Using the dimensionless variables U^* and q^* (as in equation (3)) was particularly successful in describing at-a-site variations of flow resistance. If the data under consideration include different sites, it appears to be important to include the bed slope (or energy slope) as a further factor accounting for variations in flow resistance [*Rickenmann*, 1991, 1994; *Aberle and Smart*, 2003; *Ferguson*, 2007; *David et al.*, 2010a; *Zimmermann*, 2010], although introduction of S as an additional variable did not improve the flow resistance description for the field data of *Comiti et al.* [2007]. *Ferguson* [2007] showed that in the power function equation using relative flow depth (equation (4)) the exponent b varies from a value close to 0 (Chezy equation: $b = 0$; Manning-Strickler equation: $b = 1/6$) to a value close to 1 (steep channels), with a likely smooth transition from one domain to another (as reflected by his equations (10a) and (10b)). To better investigate this transitional behavior, two slightly modified

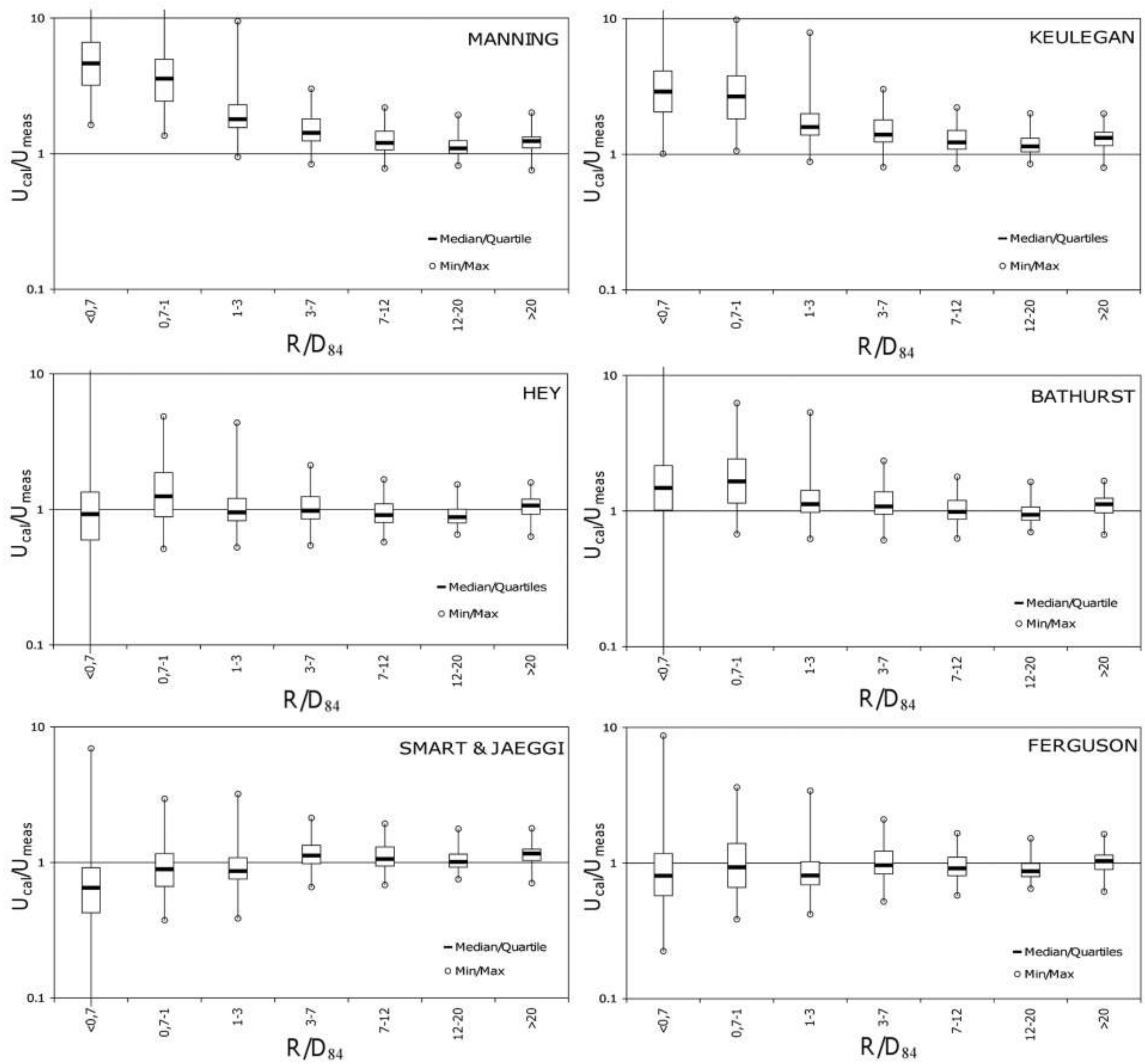

Figure 3. Results for the ratio of calculated to measured flow velocity, calculated from measured (d/D_{84}) values and shown for different classes of (R/D_{84}) values. From top to bottom, values in box plots correspond to the maximum, third quartile, median, first quartile, and minimum. Note that the Hey equation predicts negative flow velocities for 30 data points in the smallest class with $R/D_{84} < 0.7$.

dimensionless variables are introduced, namely, q^{**} and U^{**}:

$$q^{**} = \frac{q}{\sqrt{gSD_{84}^3}}, \tag{11}$$

$$U^{**} = \frac{U}{\sqrt{gSD_{84}}}. \tag{12}$$

Using these dimensionless numbers, an attempt is made to describe the data by a power function very similar to equation (3):

$$U^{**} = kq^{**^m}. \tag{13}$$

[14] It can be shown that there is a similar equivalence between (13) and (4) as there is between (3) and (4), and the same relations between the coefficients and the exponents are valid: $k = a^{(1-m)}$, $m = (2b+1)/(2b+3)$, and $b = (3m-1)/(2-2m)$. In addition, using the continuity relation $q = dU$, equation (13) can be transformed into

$$\frac{d}{D_{84}} = k^{-1} q^{**^{(1-m)}} \tag{14}$$

and into

$$U^{**} = a\left(\frac{d}{D_{84}}\right)^{\frac{m}{1-m}} = a\left(\frac{d}{D_{84}}\right)^{c}, \tag{15}$$

Table 2a. Scores (%) Obtained if Calculations Are Performed With the Measured Flow Depth d (Hydraulic Radius R)

R/D	Hey	Keulegan	Ferguson	Manning	Smart and Jäggi	Bathurst	New
			Score for $0.8 < A_r < 1.2$				
0.7	28.4	0.5	26.9	0.0	18.9	25.6	14.0
1	29.5	1.5	25.8	0.0	34.5	25.8	27.3
3	54.0	9.6	35.7	3.8	49.6	52.7	46.5
7	52.7	23.1	53.4	22.1	54.4	52.0	43.1
12	57.7	45.5	58.7	48.8	63.4	65.3	61.5
20	61.6	65.2	62.2	69.5	73.2	70.1	54.9
>100	70.3	32.4	77.1	42.6	56.1	58.0	75.5
All values	49.9	18.0	44.8	18.0	46.0	47.6	44.3
			Score for $0.5 < A_r < 1.5$				
0.7	61.0	2.9	67.4	0.0	58.1	49.2	52.3
1	60.2	10.6	72.0	1.1	84.8	45.1	78.8
3	88.0	39.9	91.1	19.0	93.4	79.3	91.9
7	89.3	58.4	91.5	57.3	85.4	79.7	89.7
12	97.7	75.1	97.7	77.9	89.7	93.9	98.6
20	99.4	86.0	99.4	87.8	93.3	95.7	100.0
>100	99.8	84.6	99.0	90.2	96.9	99.2	100.0
All values	83.5	44.3	86.9	37.4	85.1	75.5	84.9

Table 2b. Indication of the Presence or Absence of Systematic Trends of the A_r Values With One of the Listed (Input) Variables if Calculations Are Performed With the Measured Flow Depth d (Hydraulic Radius R)[a]

Variable	Hey	Smart and Jäggi	Bathurst	Ferguson	New
S	No	UU for high S	OO for high S	Slight OO for high S	Slight UU for high S
D_{84}	UU for highest D_{84}	UU for highest D_{84}	UU for highest D_{84}	UU for highest D_{84}	UU for highest D_{84}
d/D_{84}	Strong UU for lowest d/D	Strong UU for lowest d/D	Strong UU for lowest d/D	UU for lowest d/D	Strong UU for lowest d/D
W/d	No	UU for lowest W/d	No	Slight OO for very low W/d	UU for lowest W/d
q^{**}	UU for low q^{**}	No	OO for low q^{**}	Slight OO for very low q^{**}	Slight UU for very low q^{**}

[a]OO, overprediction; UU, underprediction.

Table 3a. Scores (%) Obtained if Calculations Are Performed With the Measured Flow Discharge Q or q

q^{**}	Hey	Keulegan	Ferguson	Manning	Smart and Jäggi	Bathurst	New
			Score for $0.8 < A_r < 1.2$				
0.93	57.5	2.2	57.7	19.6	53.4	46.4	55.6
2.5	65.5	8.8	65.2	54.1	55.4	56.1	65.2
30	84.7	35.8	79.5	76.8	82.7	81.0	84.6
150	71.3	57.3	79.2	66.2	81.2	75.8	78.8
400	84.6	72.6	90.5	67.2	82.6	86.6	90.0
950	86.4	79.9	91.6	64.3	88.3	90.9	89.6
30,000	91.0	78.2	94.4	84.0	90.0	92.7	94.5
All values	78.3	42.6	78.7	64.3	76.7	75.5	79.9
			Score for $0.5 < A_r < 1.5$				
0.3	95.6	23.3	93.9	55.8	97.8	79.5	97.2
0.4	97.6	47.3	98.3	89.9	99.3	90.2	98.3
0.5	99.0	82.5	99.4	98.7	100.0	96.4	99.2
0.6	100.0	90.8	100.0	100.0	100.0	100.0	100.0
0.7	100.0	100.0	100.0	100.0	100.0	100.0	100.0
0.8	100.0	100.0	100.0	100.0	100.0	100.0	100.0
1	100.0	100.0	100.0	97.6	100.0	100.0	100.0
All values	98.7	75.7	98.7	91.1	99.6	94.6	99.1

Table 3b. Indication of the Presence or Absence of Systematic Trends of the A_r Values With One of the Listed (Input) Variables if Calculations Are Performed With the Measured Flow Discharge Q or q[a]

Variable	Hey	Smart and Jäggi	Bathurst	Ferguson	New
S	No	UU for high S	OO for high S	No	No
D_{84}	UU for highest D_{84}	UU for highest D_{84}	UU for highest D_{84}	UU for highest D_{84}	UU for highest D_{84}
d/D_{84}	UU for lowest d/D	UU for lowest d/D	UU for lowest d/D	Slight UU for lowest d/D	UU for lowest d/D
W/d	OO for lowest W/d	OO for lowest W/d	UU for lowest W/d	No	No
q^{**}	No	UU for lowest q^{**}	OO for low q^{**}	Slight OO for very low q^{**}	No

[a]OO, overprediction; UU, underprediction.

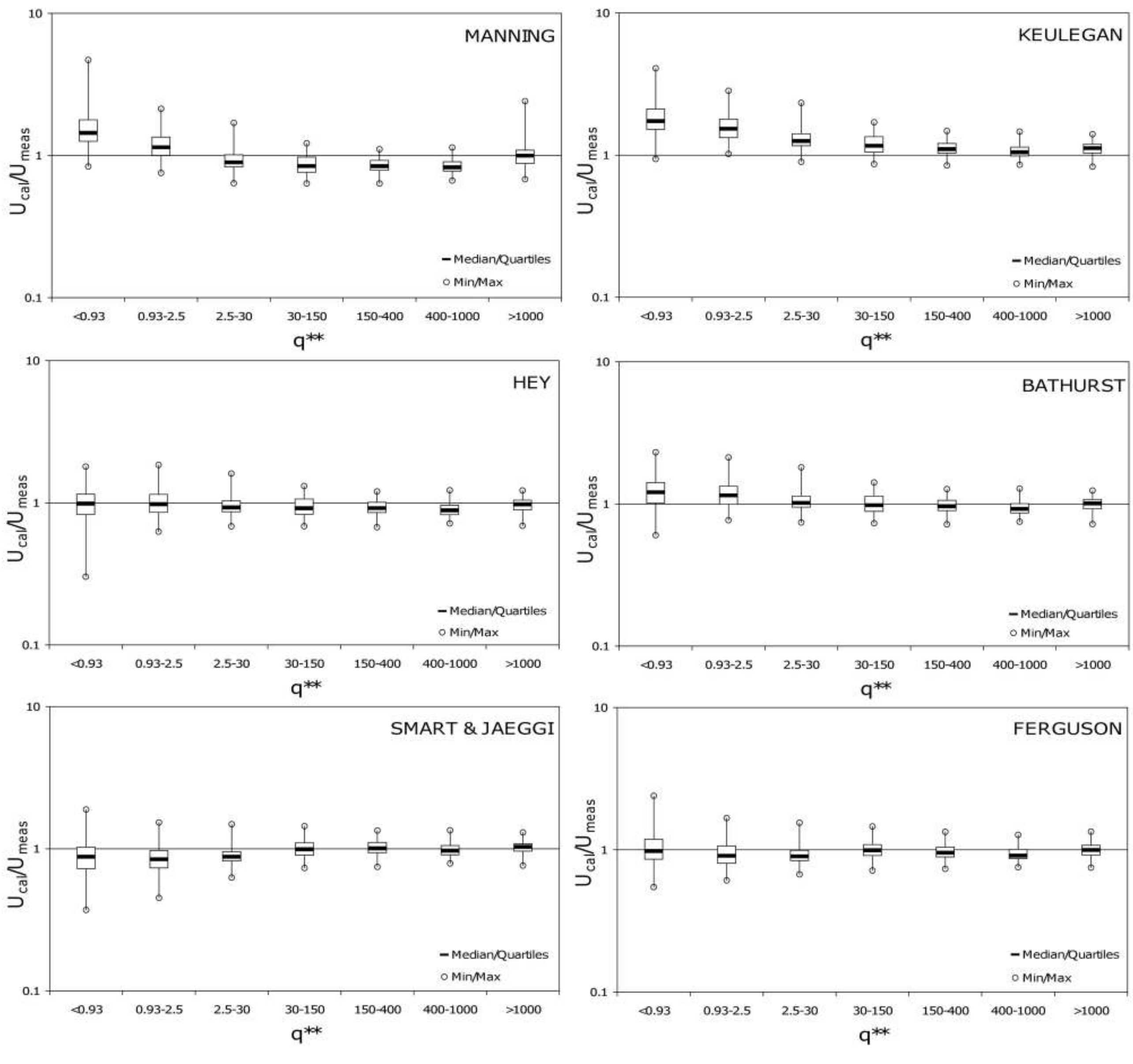

Figure 4. Results for the ratio of calculated to measured flow velocity on the basis of an iteration using flow discharge Q (equations (5)–(9), with R) and on solving the implicit equation (10b) iteratively for U^{**} using q^{**}. The ratios are shown for q^{**} classes with limits corresponding to the limits (R/D_{84}) in Figure 3 (where q^{**} is determined from d/D_{84} instead of R/D_{84}). From top to bottom, values in box plots correspond to the maximum, third quartile, median, first quartile, and minimum.

where the exponent is $c = m/(1-m)$ and, by definition, $q^{**} = U^{**}(d/D_{84})$.

3.3. New Approach Based on New Dimensionless Variables

[15] Plotting the data in Figure 5 using these dimensionless variables, there is a reasonable similarity collapse when using U^{**} and q^{**} or (d/D_{84}) and q^{**} or U^{**} and (d/D_{84}). Possible problems with spurious correlation associated with the analysis in terms of equation (13) or (14) are addressed in section 5. For decreasing values of q^{**} or (d/D_{84}), there appears to be a continuous increase of the exponent m (corresponding to an increase of the exponent b and c). This is in agreement with the observations from other studies discussed in section 3.2. As a first step toward a new flow resistance relationship, the function $U^{**} = \phi(q^{**})$ in Figure 5a is approximated for the entire data range by three power laws defined in the following domains: A, $q^{**} \leq 100$; B, $1 \leq q^{**} < 100$; C, $q^{**} < 1$. The boundary between A and B corresponds to approximately $4 < (d/D_{84}) < 7$ (Figures 5b and 5c), which is roughly equivalent to the limit between small- and intermediate-scale roughness according to *Bathurst et al.* [1981]. The boundary between B and C has been selected to obtain good power law fits in both domains; it corresponds to approximately $0.5 < (d/D_{84}) < 1$ (Figures 5b and 5c), which is loosely in agreement with the limit between intermediate- and large-scale roughness according to *Bathurst et al.* [1981]. The resulting flow resistance equations for the three domains are as follows (see also Table 4):

For $q^{**} \geq 100$

$$U^{**} = 3.20 q^{**0.395}, \tag{16a}$$

$$U/v^* = 6.84 (d/D_{84})^{0.152}, \tag{16b}$$

For $100 > q^{**} \geq 1$

$$U^{**} = 1.60 q^{**0.545}, \tag{17a}$$

$$U/v^* = 2.82 (d/D_{84})^{0.696}, \tag{17b}$$

For $1 > q^{**}$

$$U^{**} = 1.55 q^{**0.706}, \tag{18a}$$

$$U/v^* = 4.42 (d/D_{84})^{1.90}, \tag{18b}$$

For comparison, the two equations of the VPE approach of *Ferguson* [2007] are also given.

For low d/D_{84}

$$U^{**} = 1.443 q^{**0.60}, \tag{19a}$$

$$U/v^* = 2.5 (d/D_{84})^{1.0}, \tag{19b}$$

For high d/D_{84}

$$U^{**} = 3.70 q^{**0.40}, \tag{20a}$$

$$U/v^* = 6.5 (d/D_{84})^{0.167}. \tag{20b}$$

[16] Some statistical values are also given in Table 4, such as the squared correlation coefficient r^2 and the relative standard error s_e, which is defined as the standard deviation divided by the mean measured value. To obtain a smoother transition for the velocity predictions between the three domains, the logarithmic matching technique as proposed by *Guo* [2002] was used. In applying this technique, the power law equations in domains A (equation (16a) or (16b)) and C (equation (18a) or (18b)) form the end-members of a composite functional relationship $U^{**} = \phi(q^{**})$ or $U^*/v^* = \phi(d/D_{84})$, and the power law equation in domain B (equation (17a) or (17b)) is used to determine the value of the ordinate at the intersection point of the two straight lines in the log-log plot. The resulting logarithmic matching equations are

$$U^{**} = 1.5471\, q^{**0.7062} \left[1 + \left(\frac{q^{**}}{10.31}\right)^{0.6317}\right]^{-0.4930} \tag{21a}$$

$$\sqrt{\frac{8}{f}} = 4.416 \left(\frac{d}{D_{84}}\right)^{1.904} \left[1 + \left(\frac{d}{1.283\, D_{84}}\right)^{1.618}\right]^{-1.083}. \tag{21b}$$

[17] The scores of the new approach (i.e., equations (21a) and (21b)) are compared with those of the other tested equations in Tables 2a and 3a. Note that equations (5) to (9) were used with R, whereas equation (21b) was used with d because it was derived from equation (13) together with the continuity equation. The performance of the new approach is illustrated with box plots in terms of R/D classes (using equation (21b)) or of q^{**} classes (using equation (21a)) in Figure 6. Tables 2b and 3b show the presence or absence of systematic trends of the A_r values with one of the mentioned variables. The performance of the new equation (21a) in terms of q^{**} is similar to the best performing VPE equation of Ferguson (10b), except for a slightly stronger tendency of (21a) to underpredict U for the lowest (d/D_{84}) values. The performance of the new equation (21b) in terms of (d/D_{84}) is not as good as the best performing VPE equation of Ferguson (10a), but it is comparable to the performance of the Smart-Jäggi and Hey equations. A comparison of the best performing equations is also made graphically in Figure 7, where the scores are compared for the calculations based either on Q (iteration with equations (5)–(9) using R), q^{**} (equations (10b) and equation (21a)), or on (R/D). The similarity of the functional relationships of the Hey, Ferguson, and new equations are illustrated in Figure 8 for both the U^{**}–q^{**} and the $(8/f)^{0.5}$–(d/D_{84}) domains. The differences between the three relationships are most prominent in the range of small q^{**} and (d/D_{84}) values. These differences are further considered in section 5.

3.4. Explicit Form of VPE in Terms of New Dimensionless Variables

[18] The analysis in section 3.3 showed the best overall performance for the Ferguson approach, i.e., equations (10a) and (10b). To obtain an explicit equation for given discharge q, the logarithmic matching technique as proposed by *Guo* [2002] was used to substitute the implicit equation

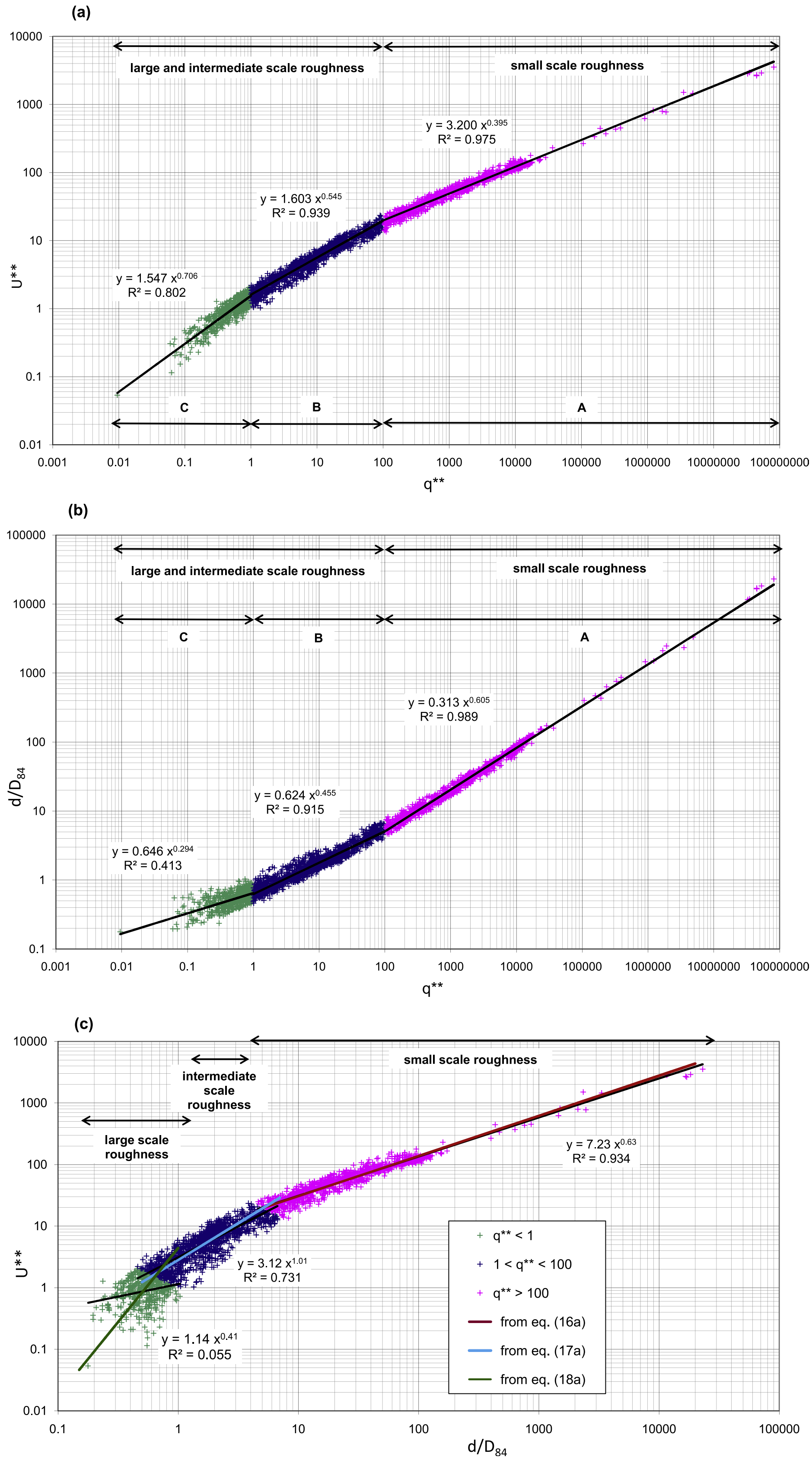

Figure 5. Comparison between dimensionless variables characterizing flow resistance: (a) U^{**} versus q^{**}, (b) (d/D_{84}) versus q^{**}, and (c) U^{**} versus (d/D_{84}).

Table 4. Statistics of New Flow Resistance Equations (16a, 17a, 18a) Derived From the 2890 Field Measurements of the Data Set[a]

Domain	N	Range of q^{**} Values	k	m	r^2 (U^{**} Versus q^{**m})	Equation	r^2 (U_{cal} Versus U_{meas})	s_e (U_{cal} Versus U_{meas})	a	b	Equation	c
A	966	$q^{**} \geq 100$	3.20	0.395	0.988	(16a)	0.906	0.122	6.84	0.152	(16b)	0.652
B	1439	$100 > q^{**} \geq 1$	1.60	0.545	0.916	(17a)	0.843	0.159	2.82	0.696	(17b)	1.196
C	485	$1 > q^{**}$	1.55	0.706	0.741	(18a)	0.848	0.208	4.42	1.90	(18b)	2.404
Ferguson, for low d/D_{84}			1.44	0.6	-	(19a)	-	-	2.5	1.0	(19b)	1.5
Ferguson, for high d/D_{84}			3.70	0.4	-	(20a)	-	-	6.5	0.167	(20b)	0.667

[a]U_{cal} refers to flow velocities calculated with equations (16a), (17a), and (18a) and U_{meas} to measured flow velocities. Also listed for comparison are the two equations proposed by Ferguson for low (19a) and (19b) and high (20a) and (20b) relative flow depth, which are the basis for eq. (10a) and (10b), using $a1 = 6.5$ and $a2 = 2.5$. The coefficients k, a, and the exponents m, b, c refer to equations (3), (4), (13), (14), and (15).

(10b). The power law equations (equation (19a) for low d/D and equation (20a) for high d/D) form the end-members of a composite functional relationship $U^{**} = \phi(q^{**})$, and equation (10b) is used to determine the value of the ordinate at the intersection point of the two straight lines in the log-log plot. The resulting logarithmic matching equation is

$$U^{**} = 1.443\, q^{**0.60} \left[1 + \left(\frac{q^{**}}{43.78}\right)^{0.8214}\right]^{-0.2435}. \qquad (22)$$

[19] For given values of q^{**} from the data set, the maximum difference between U values calculated with equations (22) and (10b) is $\pm 0.7\%$, which is considered to be acceptable for practical applications. The four significant digits for the coefficients and exponents in equation (22) are necessary to limit the error relative to equation (10a) to 1%.

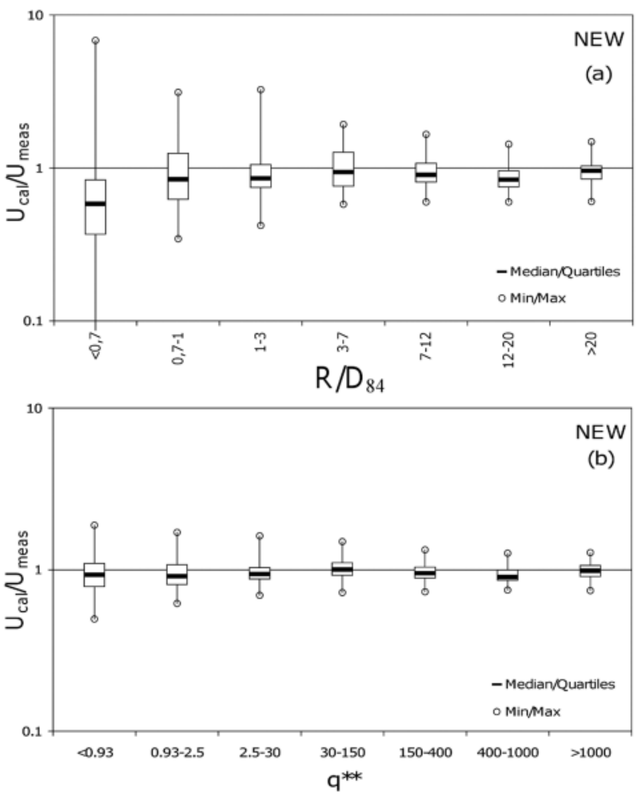

Figure 6. Results for the ratio of calculated to measured flow velocity obtained with the new approach using (a) equation (21b) with d, S, and D_{84} as input and shown versus classes of (R/D_{84}) and (b) equation (21a) with q, S, and D_{84} as input and shown versus classes of q^{**}.

4. Flow Resistance Partitioning

[20] The approach of Ferguson is used to develop a flow resistance partitioning. For domain A with small-scale roughness the resulting flow resistance equation in the form of equation (4) is close to the Manning-Strickler equation, with a value $b = 0.152 \approx 0.167$. Here the Manning-Strickler equation in the form of (20a) and (20b) as proposed by Ferguson is used to define a base level resistance for a natural streambed (the data in domain A almost exclusively include sites with $S \leq 0.01$) with a roughness value n_o, which corresponds to small-scale roughness (in the sense of *Bathurst et al.* [1981]). According to equation (20b), the Manning coefficient n_o is related to the characteristic grain size D_{84} as

$$(1/n_o) = 20.4/D_{84}{}^{0.167}. \qquad (23)$$

For the data set, D_{90} can be approximated by $D_{90} = 1.25\, D_{84}$, and equation (23) is then transformed into

$$(1/n_o) = 21.1/D_{90}{}^{0.167}. \qquad (24)$$

[21] This assumption of base level resistance represented by equation (23) or (24) is analogous to estimates of "grain" roughness in the studies of *Jäggi* [1984] and *Wong and Parker* [2006], who proposed to use an equation similar to (24) with a coefficient of 20–22 and 23.2, respectively. In the following, the dimensionless friction factor f is used to express the flow resistance partitioning, rather than using Manning's n as in some previous studies. By extrapolating equation (20a) for given q, S, and D_{84} values or (20b) for given d, S, and D_{84} values to the flows in the domains with intermediate- and large-scale roughness, a base level resistance can be calculated for these flow conditions as

$$\sqrt{\frac{8}{f_o}} = \frac{U_o(q)^{1.5}}{(gqS)^{0.5}} \qquad (25a)$$

$$\sqrt{\frac{8}{f_o}} = \frac{U_o(d)}{(gdS)^{0.5}}, \qquad (25b)$$

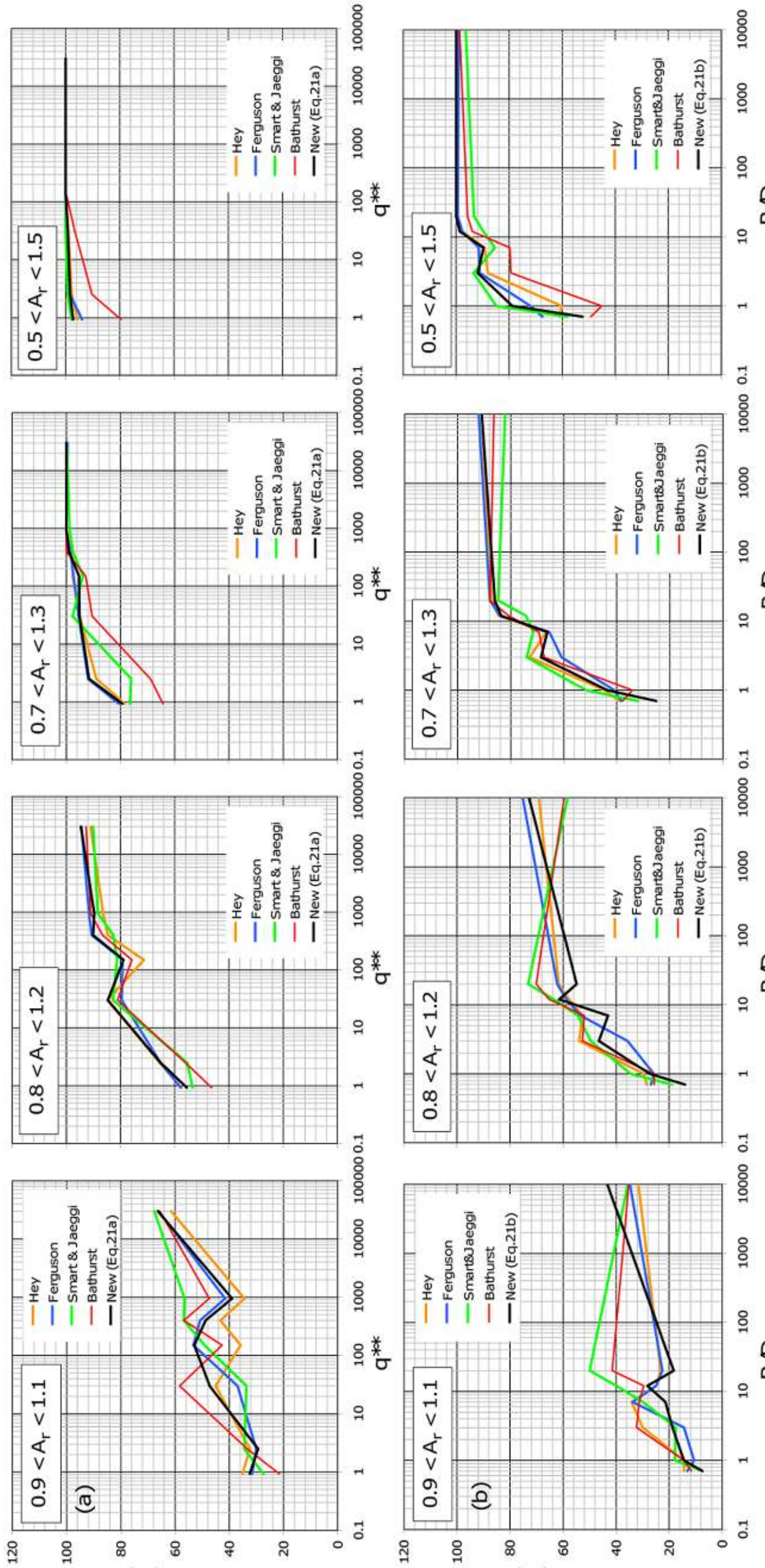

Figure 7. Comparison of scores obtained for different flow resistance equations, shown (a) versus classes of q^{**}, based on an iteration using flow discharge Q (equations (5)–(9), with R) and on solving the implicit equation (10b) iteratively for U^{**} using q^{**}, and (b) versus classes of relative depth (R/D_{84}).

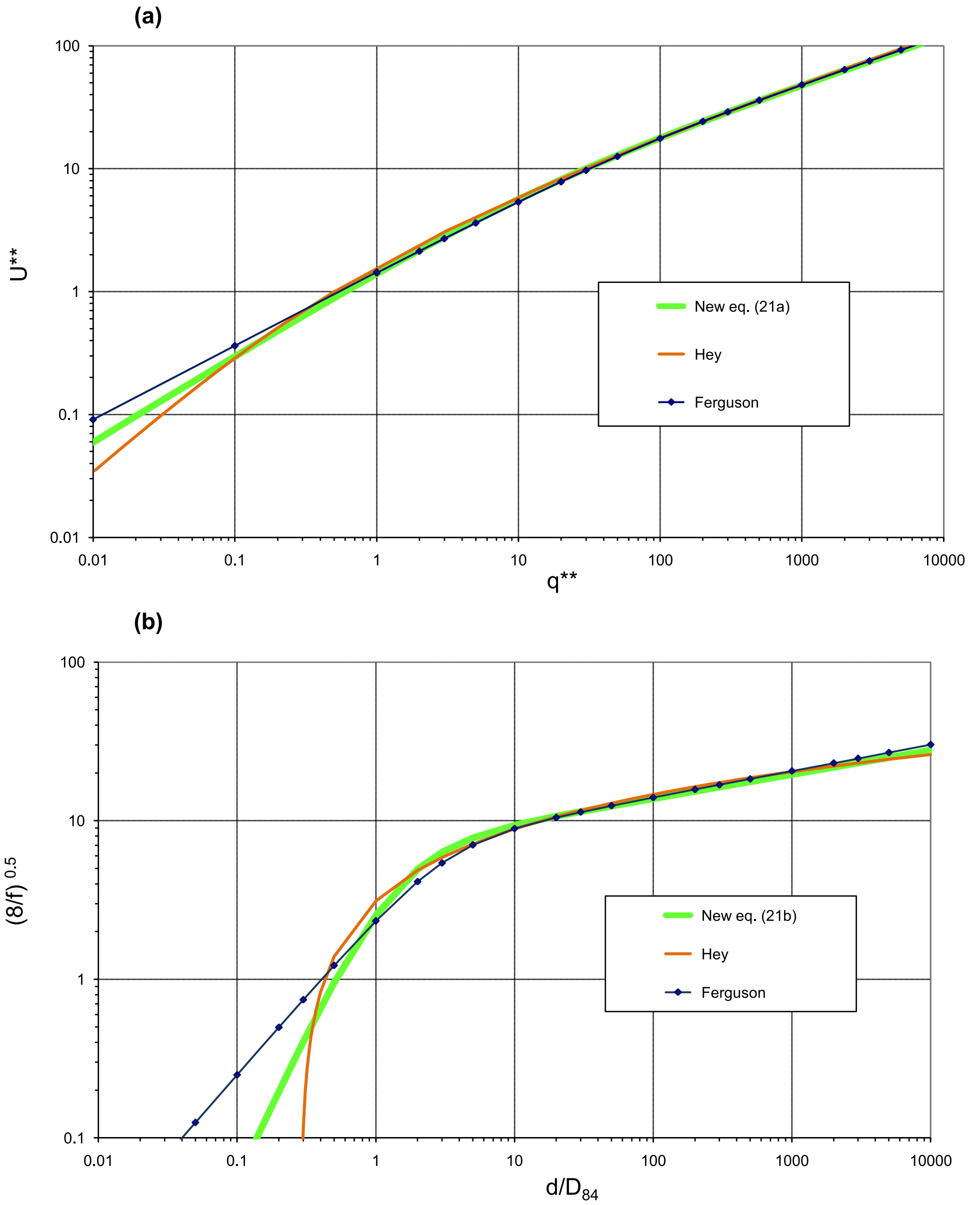

Figure 8. Comparison of the functional relationships of three flow resistance equations, shown (a) in the U^{**}–q^{**} domain and (b) in the $(8/f)^{0.5}$–(d/D_{84}) domain.

where U_o is the equivalent (virtual) velocity corresponding to base level resistance (with friction factor f_o) calculated by (20a) or (20b). Total flow resistance is calculated with the predicted velocity U using the logarithmic matching equation (22) in (26a) or the VPE (10a) in (26b):

$$\sqrt{\frac{8}{f_{\text{tot}}}} = \frac{U(q)^{1.5}}{(gqS)^{0.5}}, \tag{26a}$$

$$\sqrt{\frac{8}{f_{\text{tot}}}} = \frac{U(d)}{(gdS)^{0.5}}, \tag{26b}$$

where f_{tot} is the corresponding friction factor representing total flow resistance. Partitioning between base level (f_o) and total resistance (f_{tot}) is then simply expressed as

$$\sqrt{\frac{f_o}{f_{\text{tot}}}} = \left(\frac{U(q)}{U_o(q)}\right)^{1.5} \tag{27a}$$

$$\sqrt{\frac{f_o}{f_{\text{tot}}}} = \frac{U(d)}{U_o(d)}. \tag{27b}$$

[22] The result of applying these equations to our data is shown in Figure 9. "Macroroughness" resistance is defined here as all additional resistance other than base level resistance, and the relative proportion of macroroughness resistance is given as $1 - (f_o/f_{\text{tot}})^{0.5}$. According to Figure 9, macroroughness resistance is a function of relative flow depth, starts to become important for (d/D_{84}) smaller than about 7–10, and increases with decreasing (d/D_{84}) in a roughly semilogarithmic manner. For a further comparison

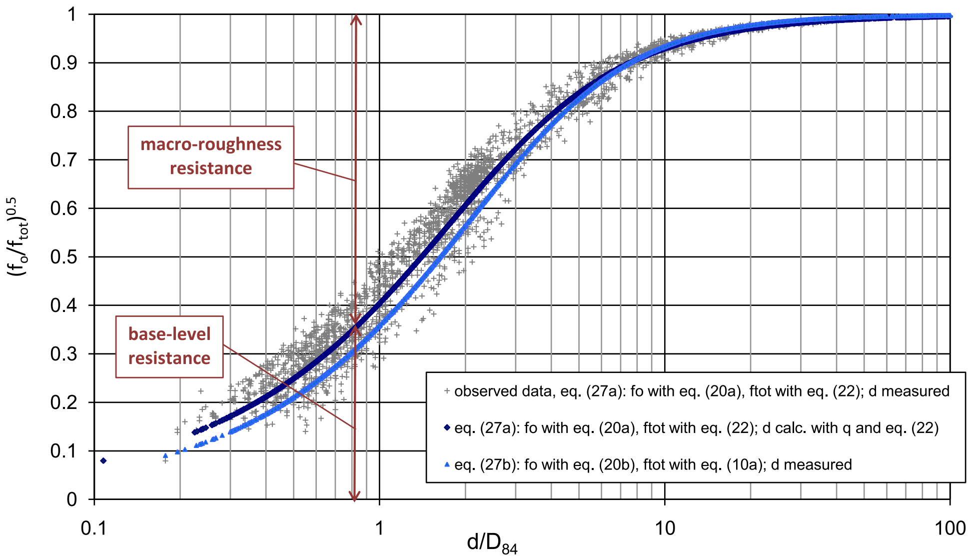

Figure 9. Flow resistance partitioning shown for the data with $(f_o/f_{tot})^{0.5}$ calculated with equations (27a) and (27b) and shown against observed flow depth d. The functional relationships are illustrated using two different calculation approaches (see legend).

(see section 5.), calculations were also made for the flow resistance partitioning in terms of Manning's n, using equations (25a), (26a), and (27a):

$$\frac{n_o}{n_{tot}} = \left(\frac{f_o}{f_{tot}}\right)^{0.5} \left(\frac{d_o}{d_{tot}}\right)^{1/6}, \tag{28}$$

where d_o was calculated with equation (20a) from q.

5. Discussion

5.1. Potential Problems With Spurious Correlation Using the New Dimensionless Variables

[23] A major advantage of the U^{**} versus q^{**} representation is that q-based equations for predicting flow velocity are more robust (less errors in the input variables) than d-based equations, especially when applied to rough steep channels [*Ferguson*, 2007; *Comiti et al.*, 2009; *Zimmermann*, 2010]. The analysis using U^{**} and q^{**} also showed how the exponent m changes with decreasing values of (d/D_{84}) or q^{**}; this cannot be easily shown with other methods. One may object that using the dimensionless numbers U^{**} and q^{**} in regression analysis introduces some degree of spurious correlation since the same variables (S, D_{84}) are contained both in the independent and dependent variables and U and q are also correlated through the continuity equation. The slope S appears on both sides in the same way only in Figure 5a (U^{**} versus q^{**}); it does not do so in Figure 5b (d/D_{84} versus q^{**}). The coefficients and exponents derived from the data shown in Figures 5a and 5b (i.e., regression equations) in terms of equations (13) and (14) are in agreement with the analytical transformation (comparing k with k^{-1} and m with $1 - m$), indicating that having S as a potential factor for spurious correlation in the analysis associated with Figure 5a is not a problem in this case. Comparing the variables (d/D_{84}) and q^{**} is equivalent to comparing U^* and q^* as used in previous studies; there is the same degree of spurious correlation in both approaches because of the continuity equation. Spurious correlation may similarly be a problem when comparing U/u^* versus (d/D_{84}), as in the more traditional flow resistance approaches (using either log laws or power laws). It is common in hydraulic analysis to use dimensionless parameters of variables based on the Buckingham pi theorem [e.g., *Yen*, 2002], which have often been used successfully to identify controlling variables on flow resistance [e.g., *Pagliara and Chiavaccini*, 2006, *Canovaro et al.*, 2007]. The good statistical performance of the new equations (16a), (17a), (18a) and the related logarithmic matching equation (21a) in terms of U_{cal} versus U_{meas} (Tables 2a, 2b, 3a, 3b, and 4 and Figures 6 and 7) supports the validity of the chosen approach. For the given values of U, d, and q a test was made by randomly assigning values of S and D_{84} from the original data set. Then the following r^2 values were obtained: in terms of U^{**} versus d/D_{84} (low expected spuriousness), $r^2 = 0.60$ for the random and $r^2 = 0.94$ for the original data set, and in terms of U^{**} versus q^{**} (high expected spuriousness), $r^2 = 0.63$ for the random and $r^2 = 0.90$ for the original data set. The similar change in the correlation coefficient suggests that the spurious correlation is not a major problem.

5.2. Flow Resistance for Intermediate- and Large-Scale Roughness

[24] A power law flow resistance equation (equation (19b)) was proposed for low d/D values by *Ferguson* [2007]. A slightly modified analysis using U^{**} and q^{**} can result in a very similar flow resistance equation for large-scale roughness. For very low values of d/D_{84}, the transformation between equations (13) and (14) via the continuity equation may no longer be strictly valid if a part of the channel width is occupied by larger grains and the true average bed level for zero flow depth is not exactly known. Therefore, only data with approximately $d/D_{84} > 0.5$ are considered, as illustrated in Figure 10. On the basis of

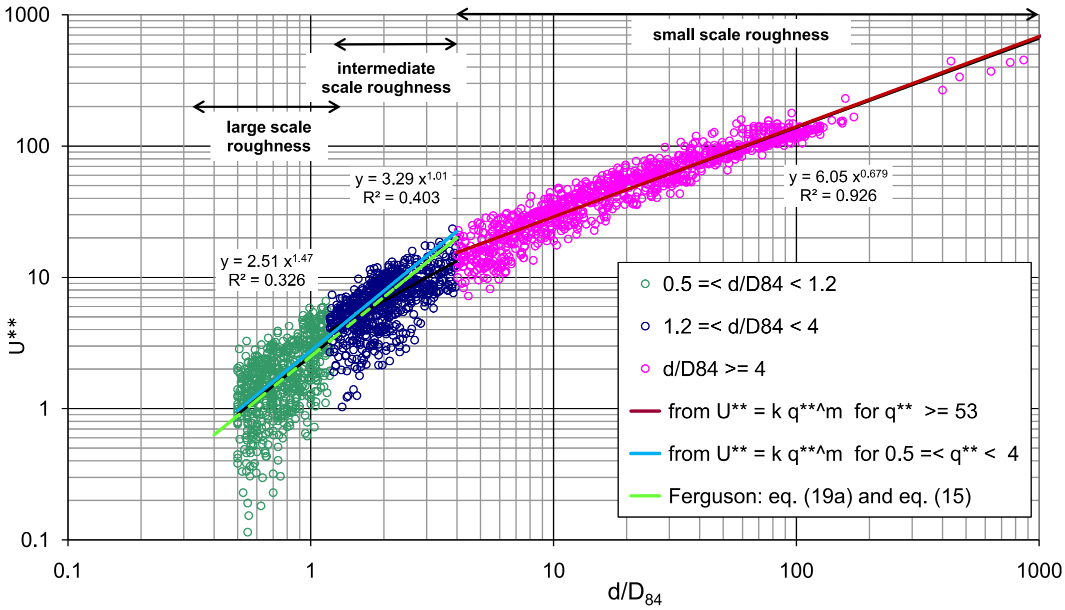

Figure 10. Comparison of flow resistance relationships in the U^{**}–(d/D_{84}) domain, excluding data with very small values of $d/D_{84} < 0.5$, for which the application of the continuity equation may be problematic.

equation (21a) the limits for $d/D_{84} = 0.5$, 1.2, and 4 correspond approximately to $q^{**} = 0.5$, 4, and 53, respectively. Figure 10 uses the dimensionless variables U^{**} and (d/D_{84}), so the potential problem with spurious correlation is limited to having D_{84} in both variables. Considering the range $0.5 < d/D_{84} \leq 1.2$, i.e., large-scale roughness, the regression of U^{**} versus (d/D_{84}) results in an equation very similar to the one proposed by *Ferguson* [2007] for low d/D, i.e., equation (19a) transformed with equation (15). Similarly, if a regression equation of U^{**} versus q^{**} determined for the range $0.5 < q^{**} < 4$ (large-scale roughness) is transformed into the domain U^{**} versus (d/D_{84}), the resulting equation is again very similar to the equation proposed by *Ferguson* [2007] for low d/D values (Figure 10). This modified analysis and the comparison of Figures 10 and 5c show that the exclusion of data with $d/D_{84} < 0.5$ has important implications on the flow resistance functions for the large-scale roughness domain.

[25] The analysis using U^{**} and q^{**} in section 3. (Figure 5) showed that the exponent m (and thus also the bed slope exponent in equation (3)) increases with decreasing values of q^{**} or d/D_{84}; this cannot be easily shown with other methods. As a result, the Manning-Strickler equation appears to be unsuitable for small relative flow depths in the domain of intermediate- and large-scale roughness, confirming the conclusion of *Ferguson* [2010]. Some previous studies also found that when using a U^*–q^* relation (or a relation where U equals the function of (Q, S, D_{90})) and comparing different sites, the inclusion of the bed slope with a positive exponent as an additional factor in the power law formulation in the form of equation (3) improved the flow velocity predictions [*Rickenmann* 1991, 1994; *Aberle and Smart*, 2003; *Ferguson*, 2007; *Zimmermann*, 2010]. However, other studies related to flows in steep channels concluded that bed slope was not important or that a negative bed slope exponent was required to achieve better flow velocity predictions (summarized by *Comiti et al.* [2007]).

[26] The traditional logarithmic flow resistance equation of Hey (equation (7)) and two power law approaches (the Ferguson VPE equations (10a) and (10b) and the new approach equations (21a) and (21b)) are also compared in Figure 8 in addition to Figures 3, 4, and 7. It is evident that the Hey equation provides a good representation of the mean trend of the data for most of the range of the examined flow conditions. However, a more detailed inspection (e.g., Figure 3) shows that that the Hey equation results in an overprediction of U for R/D_{84} values close to 1 and in an underprediction of U for $R/D_{84} < 0.5$. The estimation of the mean velocity with a logarithmic flow resistance equation appears to be reasonable for $R/D_{84} > 1.2$, i.e., small- and intermediate-scale roughness. Although velocity profiles in the intermediate-scale roughness domain may deviate considerably from logarithmic [*Bathurst*, 1985; *Wiberg and Smith*, 1991], several studies demonstrated that logarithmic resistance equations still provide adequate predictions [*Ferguson*, 2007].

5.3. Flow Resistance Variation at a Site

[27] The data set of this study includes measurements taken at a given site or reach for varying flow discharges, and together with data from many different sites, the comparison of all measurements represents a combination of flow resistance variation both at a site and between sites. Figures 11a and 11b represent some of the data shown in Figure 5 with a separate identification of some sites or reaches for which measurements include varying discharge conditions. Despite some scatter of the at-a-site measurements, these data generally follow the same mean trend (i.e., having the same exponent m or c as defined by the bulk of the data), but indicating some variation of the coefficient k or a, which may be site specific. The three at-a-site

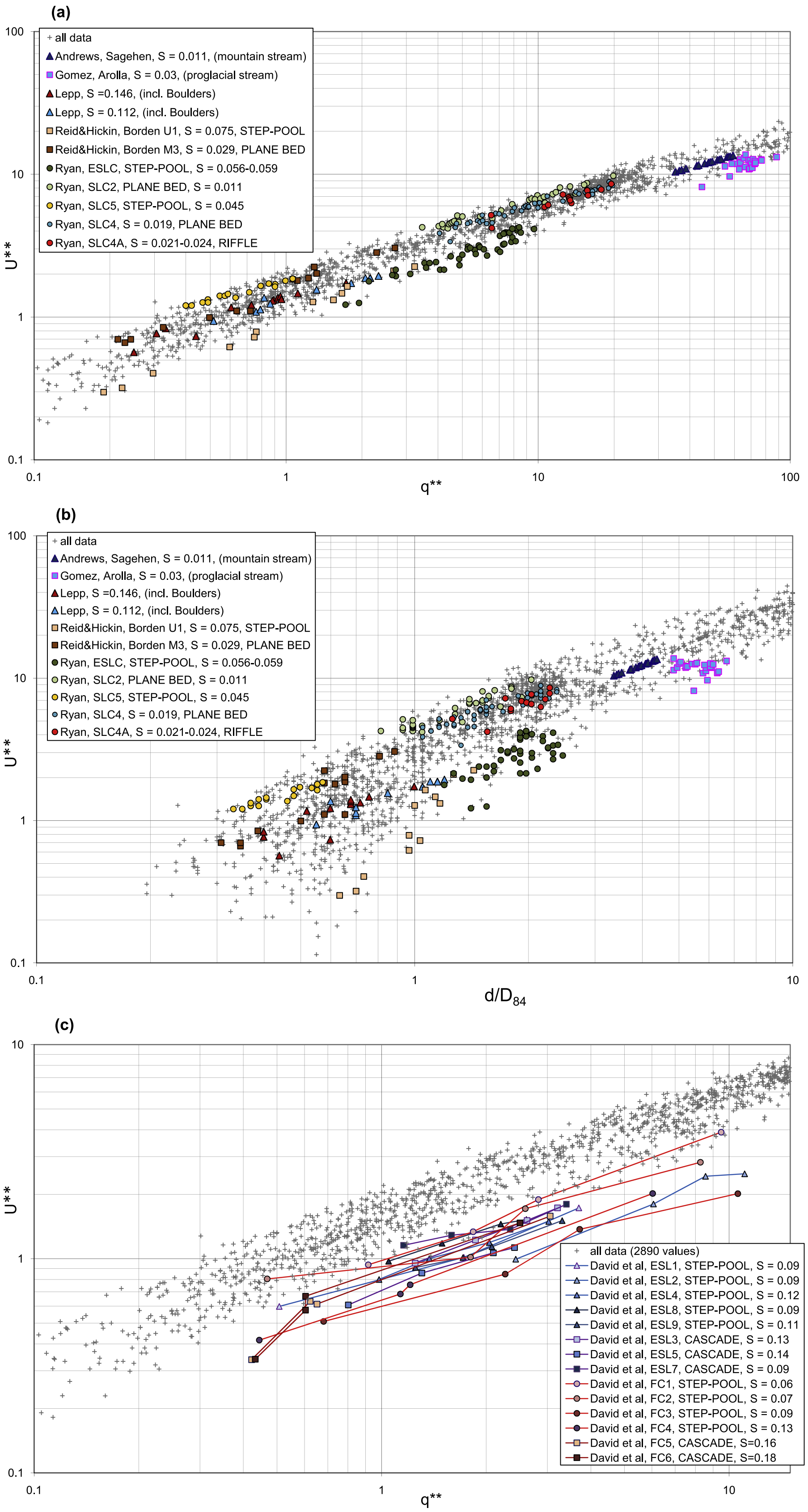

Figure 11. Comparison of some at-a-site data with the general trend of flow resistance defined by the entire data set, including also between-site variation, shown (a) in the U^{**}–q^{**} domain and (b) in the U^{**}–(d/D_{84}) domain. (c) The data of *David et al.* [2010a] are shown additionally which were not included in the reduced data set of 2890 values used for the evaluation of the flow resistance equations.

sets characterized as "plane beds" plot at the upper end of the range and appear to be associated with a relatively larger coefficient k than two at-a-site sets with "step-pool" bed morphology (*Reid and Hickin* [2008], Borden U1, and *Ryan et al.* [2002], ESLC, in Figure 11), which plot at the lower end of the range. However, there is also a step-pool data set (*Ryan et al.* [2002], SLC5, in Figure 11) that is not in agreement with the above trend. There is also some trend that for a given range of q^{**} or (d/D_{84}) values, channel sites or reaches with a larger bed slope appear to have a somewhat higher flow resistance (i.e., a smaller coefficient k) than those with a smaller bed slope. This trend (although it is not consistent) is in qualitative agreement with the flow resistance equation of *Smart and Jäggi* [1983] for approximately $(d/D_{84}) < 10$ (Figure 2). In general, the variation of the data around the mean trend increases with decreasing relative flow depth. The higher flow resistance at steeper slopes is also confirmed from other studies in terms of U/u^* versus (d/D_{84}) [*Mussetter*, 1989; *Marcus et al.*, 1992; *Bathurst*, 2002] and in terms of U^* versus q^* in the Rio Cordon [*Comiti et al.*, 2007].

[28] At the East St. Louis Creek and at Fool Creek, *David et al.* [2010a, 2010b] made more than 50 measurements of flow resistance in step-pool and cascade reaches (Table 1). These data were not included in the evaluation of the equations because flow depth is not reported. However, they are shown in Figure 11c. The data of David et al. plot generally below the other data, implying higher flow resistance for the comparatively steep step-pool and cascade reaches. These channel reaches also include large woody debris, and *David et al.* [2010a, 2010b] found flow resistance to increase with increasing wood load. In terms of the exponent m these data generally follow the same mean trend defined by equation (10b) or (22). The roughly parallel alignment of the data of different reaches indicates again a variation of the coefficient k between sites, which is analogous to a variation of the representative bed roughness k_s in equation (2). For given q^{**} values, there is some trend for reaches with larger bed slopes to have smaller k values, but as for the other data this trend is not consistent. These observations are in agreement with a conclusion by *David et al.* [2010a, 2010b] that the variables q^* and S largely control flow resistance in their study reaches.

[29] For flume experiments replicating flow conditions in the Rio Cordon, *Comiti et al.* [2009] showed that the exponent m for the nappe flow regime, including tumbling flow, was close to 1, whereas for skimming flow, m was smaller. This change suggests that once steps are drowned out, spill resistance may disappear and the flow resistance is more similar to smoother beds. It also indicates that k and m may change somewhat with changing flow intensity for at-a-site flow resistance. *Zimmermann* [2010] performed 205 flume experiments on flow resistance in steep channels, including a wide range of flow conditions with bed slopes from 0.03 to 0.23 and relative depths from 0.44 to 6.5. He fitted his at-a-site data to a relation similar to equation (3) but with independent exponents for q^* and S, and he found that the hydraulic geometry approach using U^*, q^*, and S collapses much of the variability of his flow conditions, which varied between wake-dominated flows (which were more common in the wide, low-gradient experiments) and spill-dominated flows associated with water plunging over steps into pools. He also tested the dimensionless hydraulic geometry relation (3) with a fixed exponent $m = 0.6$ and found nearly as good results as for the approach using both q^* and S as independent variables. *Zimmermann* [2010] did not find any clear effect of step-pool geometric parameters on flow resistance (apart from their number), confirming the unsuccessful attempts of *Comiti et al.* [2007, 2009] to model in detail effects of step-pool bed morphology on flow resistance. *Zimmermann* [2010] speculated that steep streams may follow regime equations (i.e., power law equations between flow velocity or flow depth or width as an dependent variable and discharge as an independent variable), which is also suggested by other studies [*Kellerhals*, 1970; *Beven et al.*, 1979].

5.4. Flow Resistance Partitioning and Bed Load Transport Predictions

[30] The concept of flow resistance partitioning was first proposed for application in large lowland rivers with large relative flow depths [*Einstein and Barbarossa*, 1952]. Total flow resistance in gravel bed streams has been divided into form and grain resistance [*Meyer-Peter and Müller*, 1948; *Parker and Peterson*, 1980; *Carson and Griffiths*, 1987; *Carson*, 1987; *Gomez and Church*, 1989; *Millar and Quick*, 1994; *Millar* 1999], and only the latter part should be taken into account for the bed load transport calculations. *Millar* [1999] proposed that grain resistance may be evaluated using the logarithmic equation proposed by Keulegan (equation (6)), which is based on D_{50}. To estimate grain resistance, equation (6) has also been applied in many other studies [*Curran and Wohl*, 2003; *MacFarlane and Wohl*, 2003; *Comiti et al.*, 2007, 2009; *Reid and Hickin*, 2008; *David et al.*, 2011]. Compared to using equations (20a) and (20b) to define an average resistance level as a base level resistance, equation (6) would represent a lower bound of observed flow resistance (i.e., friction factor) for flows with small-scale roughness.

[31] From his flume experiments on flow resistance in steep channels including a wide range of flow conditions, *Zimmermann* [2010] concluded that the traditional concept of separating grain and form resistance does not make sense for shallow flows in steep streams. Indeed, in steep and rough streams it appears to be difficult to distinguish between grain and "form" resistance (the latter term including also other sources of resistance, such as spill drag, variation in cross-section geometry and flow width, woody debris, etc.) since larger particles are part of the bed material, of macroroughness elements, and of the bank and may contribute in varying degrees to different types of resistance. However, the importance of accounting for additional energy "losses" or increased total flow resistance in steep streams (as compared with lowland rivers) in the context of bed load transport calculations has been pointed out in several studies [*Govers and Rauws*, 1986; *Rauws*, 1988; *Palt*, 2001; *Rickenmann*, 2001, 2005; *Yager et al.*, 2007; *Chiari et al.*, 2010; *Rickenmann and Koschni*, 2010; *Zimmermann*, 2010]. In some of these studies, similar concepts to the grain and form resistance partitioning in lowland rivers were also applied in steep streams with some success [*Govers and Rauws*, 1986; *Rauws*, 1988; *Palt*, 2001;

Rickenmann, 2005; *Rickenmann et al.*, 2006; *Yager et al.*, 2007; *Chiari et al.*, 2010]. Many bed load transport equations were developed and calibrated with flume experiments, where grain flow resistance may have been prevalent or where macroroughness bed elements and low relative depths were largely absent. Therefore, sediment transport rates in steep streams may be overestimated using traditional sediment transport formulas because most of the flow energy in steep streams is lost to form and spill drag [*Rickenmann*, 2001; *Zimmermann*, 2010]. Several studies showed that the mean flow velocity and turbulence intensity near the bed decrease with decreasing relative depth *R*/*D* [*Bayazit*, 1976; *Carollo et al.*, 2005; *Dietrich and Koll*, 1997; *Lamb et al.*, 2008; *Tsujimoto*, 1991; *Wang et al.*, 1993]. These changes in turbulence properties were observed with uniform and nonuniform sediments, and they refer to flow characteristics in the intermediate- and large-scale roughness domain that may be effective in reducing bed load transport in steep and rough streams. On the other hand, the overestimation of sediment transport in steep streams may also be due to limited sediment supply [*D'Agostino and Lenzi*, 1999; *Lenzi et al.*, 2004; *Turowski et al.*, 2009].

[32] In the light of this discussion, some of the previous approaches to correct for overestimation of bed load transport [e.g., *Palt*, 2001; *Rickenmann*, 2005; *Chiari et al.*, 2010] can be considered as an attempt to separate between a base level and macroroughness (sum of additional) flow resistance, the latter type typically not being taken into account with traditional bed load transport formulas. The terminology of grain and form resistance partitioning as it was used in these studies appears to be incorrect, although the selected approach may still be valid. *Pagliara and Chiavaccini* [2006] determined resistance associated with "smaller" grains and total flow resistance separately in flume experiments for varying boulder concentrations up to 30% and channel gradients up to $S = 0.25$. Using their results, additional flow resistance due to the boulders in terms of $(f_o/f_{\mathrm{tot}})^{0.5}$ accounts for approximately 40%–50% for a step-pool-like boulder arrangement [*Chiari*, 2008]. *Church and Zimmermann* [2007] summarize evidence that macroroughness (or additional) flow resistance may account for about 45%–90% of the total flow resistance in terms of $(f_o/f_{\mathrm{tot}})^{0.5}$ in boulder-dominated streams. Similarly high proportions of flow resistance of form and spill resistance in relation to total flow resistance are reported for flume experiments by *Comiti et al.* [2009] that consider step-pool structures and by *Wilcox et al.* [2006] that consider steps and large woody debris.

[33] On the basis of independent measurements of flow resistance, *Palt* [2001] proposed equation (29) and *Chiari et al.* [2010] proposed equation (30) for the flow resistance partitioning:

$$\frac{n_o}{n_{\mathrm{tot}}} = 0.13\, S^{-0.28} \left(\frac{d}{D_{90}}\right)^{0.21}, \tag{29}$$

$$\frac{n_o}{n_{\mathrm{tot}}} = 0.092\, S^{-0.35} \left(\frac{d}{D_{90}}\right)^{0.33}. \tag{30}$$

[34] Flow resistance partitioning for the data of this study in terms of (n_o/n_{tot}) is shown versus the bed slope in Figure 12, where (n_o/n_{tot}) was calculated with the approach proposed in this study (equations (22), (27a), and (28)) and compared to calculations using both equation (29) and (30).

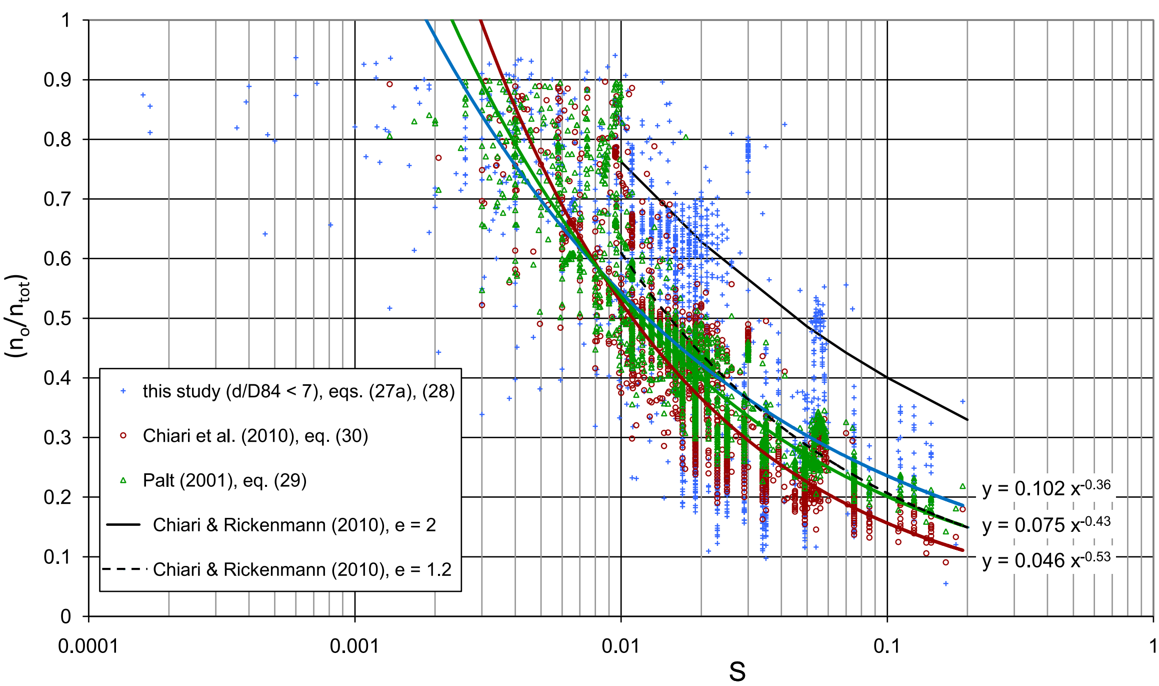

Figure 12. Flow resistance partitioning calculated for our data with several equations based on flow resistance data shown versus bed slope. The power law equations refer to the colored trend lines. The black trend lines are based on a back calculation of flow resistance partitioning based on bed load data.

The three approaches result in a similar variation of (n_o/n_{tot}) values, and similar trend lines for power law functions of (n_o/n_{tot}) versus S are obtained:

$$\frac{n_o}{n_{\mathrm{tot}}} = p\, S^{-z}, \tag{31}$$

where the corresponding coefficients p and exponents z are shown in Figure 12.

[35] Adapting the approaches of *Meyer-Peter and Müller* [1948] and *Palt* [2001], *Chiari et al.* [2010] and *Chiari and Rickenmann* [2011] calculated bed load transport with a reduced energy slope S_o expressed as

$$\frac{S_o}{S} = \left(\frac{n_o}{n_{\mathrm{tot}}}\right)^e, \tag{32}$$

where the exponent e is in the range 1.33–2 according to *Meyer-Peter and Müller* [1948] and S_o corresponds to the base level friction f_o or n_o. For their flume bed load transport data, Meyer-Peter and Müller determined a best fit exponent of $e = 1.5$. Using equations (30) and (32), back estimation of e from bed load data for the Austrian and Swiss flood events in 2005 resulted in a best fit exponent e in the range of about 1.2–1.5 [*Chiari*, 2008; *Chiari and Rickenmann*, 2011]. Using the same bed load data, a back estimation of the functional relationship (31) was also made with (32), without using an explicit flow resistance partitioning such as equations (27), (29), and (30) [*Chiari and Rickenmann*, 2011]. The corresponding power function trend lines for (n_o/n_{tot}) as a function of S (equation (31)) are given with $p = 0.21$ and $z = 0.28$ for $e = 2$ and $p = 0.07$ and $z = 0.47$ for $e = 1.2$. These power laws are also indicated in Figure 12. This comparison supports the findings of several studies in which accounting for macroroughness (additional) resistance in mountain streams resulted in much better agreement between predicted and observed bed load volumes for flood events in 2005 in Austrian and Swiss torrents and mountain rivers [*Rickenmann et al.*, 2006; *Chiari*, 2008; *Chiari et al.*, 2010; *Chiari and Rickenmann*, 2011] and for flood events in 2000 in mountain rivers in southwestern Switzerland [*Badoux and Rickenmann*, 2008]. Similarly, using total flow resistance measurements and an estimate of grain (base level) resistance similar to equation (24) to account for additional (macroroughness) resistance, *Palt* [2001] applied equation (32) with $e = 2$ and found much better agreement between his bed load measurements in Himalayan rivers and the bed load transport formulas of *Meyer-Peter and Müller* [1948], *Smart and Jäggi* [1983], and *Rickenmann* [1991].

[36] A caveat is in place when applying the proposed partitioning of flow resistance (equation (22) or (10a) with (27a) or (27b)) to flume conditions with very high sediment concentrations but no macroroughness elements. Such conditions were present in the experiments of *Smart and Jäggi* [1983] and *Rickenmann* [1991], with all particle sizes of the mobile bed being in motion. Application of equations (24) and (25) to these experiments resulted in an implausible reduction of calculated bed load transport rates [*Rickenmann*, 2011]. This effect is partly due to unrealistic (too small) flow depths being calculated with a q-based approach using $d = q/U$, while in reality measured flow depths were considerably larger because of very high sediment concentrations.

6. Conclusions

[37] A data set consisting of 2890 field measurements covering a wide range of bed slopes, grain diameters, flow discharges, and river widths was used to test the suitability of several conventional flow resistance equations to predict the mean flow velocity. The Manning-Strickler, Keulegan, Smart-Jäggi, Hey, Bathurst, and Ferguson equations and a new equation were considered. The equations are based on either flume or field measurements or a combination of both. The equations were evaluated both with flow depth as input and with discharge as input, which typically requires iterative calculations. The tests demonstrated that some equations should be used with caution, especially in the intermediate- and the large-scale roughness domains with small relative flow depths [*Bathurst et al.*, 1981]. The Manning-Strickler equation appears to be unsuitable in this range of flow conditions. Generally, a much better prediction was obtained with all equations when the flow discharge Q or q was used as an input parameter instead of the relative depth d/D. However, for small relative depths most equations yield a systematic deviation between predicted and observed velocity. The best overall performance for flow resistance prediction was obtained with the VPE approach of *Ferguson* [2007]. Introducing new dimensionless variables U^{**} and q^{**} in terms of nondimensional hydraulic geometry equations (equations (13) and (14)) resulted in a similarity collapse for the entire data range. Using a logarithmic matching method, the dimensionless variables allowed proposing an explicit equation of Ferguson's VPE approach.

[38] These dimensionless variables were further used to discuss how a power law flow resistance equation varies over three domains, approximately reflecting the three roughness scales proposed by *Bathurst et al.* [1981]. The dimensionless variables were also useful for considering the limitations related to the development of a q-based approach at very low relative flow depths if the true average bed level for zero flow depth is not exactly known in the presence of large grains. The presented analysis suggests that between-site and at-a-site variations of flow resistance have strong similarities. On the basis of the Ferguson approach, a flow resistance partitioning method was presented to account for high flow resistance in the domains of intermediate- and large-scale roughness in natural gravel, cobble, and boulder bed streams, and this method was compared with similar approaches.

[39] **Acknowledgments.** This study was supported by Cemagref, the WSL, ANR project ANR-09-RISK-004/GESTRANS of the French National Research Agency (grant to A.R.), and the CCES-APUNCH project of the Swiss Federal Institutes of Technology (grant to D.R.). We thank two anonymous reviewers and Gabrielle David for their constructive comments, which helped to improve the manuscript.

References

Aberle, J., and G. M. Smart (2003), The influence of roughness structure on flow resistance on steep slopes, *J. Hydraul. Res.*, *41*, 259–269.

Adenlof, K. A., and E. E. Wohl (1994), Controls on bedload movement in a subalpine stream of the Colorado Rocky Mountains, U.S.A., *Arct. Alp. Res.*, *26*, 77–85.

Andrews, E. D. (1994), Marginal bed load transport in a gravel bed stream, Sagehen Creek, California, *Water Resour. Res.*, *30*, 2241–2250, doi:10.1029/94WR00553.
Badoux, A., and D. Rickenmann (2008), Berechnungen zum Geschiebetransport während der Hochwasser 1993 und 2000 im Wallis, *Wasser Energie Luft*, *100*, 217–226.
Barnes, H. H. (1967), Roughness characteristics of natural channels, *U.S. Geol. Surv. Water Supply Pap.*, *1849*, 213 pp.
Bathurst, J. C. (1978), Flow resistance of large-scale roughness, *J. Hydraul. Div. Am. Soc. Civ. Eng.*, *104*, 1587–1603.
Bathurst, J. C. (1985), Flow resistance estimation in mountain rivers, *J. Hydraul. Eng.*, *111*, 625–643.
Bathurst, J. C. (2002), At-a-site variation and minimum flow resistance for mountain rivers. *J. Hydrol.*, *269*, 11–26.
Bathurst, J. C., R.-M. Li, and D. B. Simons (1981), Resistance equation for large-scale roughness, *J. Hydraul. Div. Am. Soc. Civ. Eng.*, *107*, 1593–1613.
Bayazit, M. (1976), Free surface flow in a channel of large relative roughness, *J. Hydraul. Res.*, *14*, 115–126.
Beven, K., K. Gilman, and M. Newson (1979), Flow and flow routing in upland channel networks, *Hydrol. Sci. Bull.*, *24*, 303–325.
Bray, D. I. (1979), Estimating average velocity in gravel-bed rivers, *J. Hydraul. Div. Am. Soc. Civ. Eng.*, *105*, 1103–1122.
Canovaro, F., E. Paris, and L. Solari (2007), Effects of macro-scale bed roughness geometry on flow resistance, *Water Resour. Res.*, *43*, W10414, doi:10.1029/2006WR005727.
Carollo, F. G., V. Fero, and D. Termini (2005), Analyzing turbulence intensity in gravel bed channels, *J. Hydraul. Eng.*, *131*, 1050–1061.
Carson, M. A. (1987), Measures of flow intensity as predictors of bed load, *J. Hydraul. Eng.*, *113*, 1402–1421.
Carson, M. A., and G. A. Griffiths (1987), Bedload transport in gravel channels, *J. Hydrol. N. Z.*, *26*(1), 151 pp.
Chiari, M. (2008), Numerical modelling of bedload transport in torrents and mountain streams, Ph.D. dissertation, Inst. für Alp. Naturgefahren, Univ. für Bodenkultur Wien, Vienna.
Chiari, M., and D. Rickenmann (2011), Back-calculation of bedload transport in steep channels with a numerical model, *Earth Surf. Processes Landforms*, *36*, 805–815, doi:10.1002/esp.2108.
Chiari, M., K. Friedl, and D. Rickenmann (2010), A one dimensional bedload transport model for steep slopes, *J. Hydraul. Res.*, *48*, 152–160.
Church, M., and K. Rood (1983), *Catalogue of Alluvial River Channel Regime Data*, 99 pp., Dep. of Geogr., Univ. of B. C., Vancouver, B. C., Canada.
Church, M., and A. Zimmermann (2007), Form and stability of step-pool channels: Research progress, *Water Resour. Res.*, *43*, W03415, doi:10.1029/2006WR005037.
Colosimo, C., V. Copertino, and M. Veltri (1988), Friction factor evaluation in gravel-bed rivers, *J. Hydraul. Eng.*, *114*, 861–876.
Comiti, F., L. Mao, A. Wilcox, E. Wohl, and M. Lenzi (2007), Field-derived relationships for flow velocity and resistance in high-gradient streams, *J. Hydrol.*, *340*, 48–62, doi:10.1016/j.jhydrol.2007.03.021.
Comiti, F., D. Cadol, and E. Wohl (2009), Flow regimes, bed morphology and flow resistance in self-formed step-pool channels, *Water Resour. Res.*, *45*, W04424, doi:10.1029/2008WR007259.
Coon, W. F. (1998), Estimation of roughness coefficients for natural stream channels with vegetated banks, *U.S. Geol. Surv. Water Supply Pap.*, *2441*, 133 pp.
Curran, J. H., and E. E. Wohl (2003), Large woody debris and flow resistance in step-pool channels, Cascade Range, Washington, *Geomorphology*, *51*, 141–157, doi:10.1016/S0169-555X(02)00333-1.
D'Agostino, V., and M. A. Lenzi (1999), Bedload transport in the instrumented catchment of the Rio Cordon: Part II. Analysis of the bedload rate, *Catena*, *36*, 191–204.
David, G. C. L., E. E. Wohl, S. E. Yochum, and B. P. Bledsoe (2010a), Controls on spatial variations in flow resistance along steep mountain streams, *Water Resour. Res.*, *46*, W03513, doi:10.1029/2009WR008134.
David, G. C. L., E. E. Wohl, S. E. Yochum, and B. P. Bledsoe (2010b), Controls on at-a-station hydraulic geometry relationships in steep headwater streams, *Earth Surf. Processes Landforms*, *35*, 1820–1837, doi:10.1002/esp.2023.
David, G. C. L., E. E. Wohl, S. E. Yochum, and B. P. Bledsoe (2011), Comparative analysis of bed resistance partitioning in high gradient streams, *Water Resour. Res.*, doi:10.1029/2010WR009540, in press.
Dietrich, A., and K. Koll (1997), Velocity field and resistance of flow over rough surfaces with large and small relative submergence, *Int. J. Sed. Res.*, *12*, 21–33.
Einstein, H. A., and N. L. Barbarossa (1952), River channel roughness, *Trans. Am. Soc. Civ. Eng.*, *117*, 1121–1146.
Ferguson, R. (2007), Flow resistance equations for gravel and boulder bed streams, *Water Resour. Res.*, *43*, W05427, 1–12, doi:10.1029/2006WR005422.
Ferguson, R. (2010), Time to abandon the Manning equation?, *Earth Surf. Processes Landforms*, *35*, 1873–1876.
Gomez, B. (1988), Two data sets describing channel-wide temporal variations in bedload-transport rates, Denver, Colorado, *U.S. Geol. Surv. Open File Rep.*, *88–88*, 26 pp.
Gomez, B., and M. Church (1989), An assessment of bedload sediment transport formulae for gravel bed rivers, *Water Resour. Res.*, *25*, 1161–1186.
Govers, G., and G. Rauws (1986), Transporting capacity of overland flow on plane and on irregular beds, *Earth Surf. Processes Landforms*, *11*, 515–524.
Griffiths, G. (1981), Flow resistance in coarse gravel bed rivers, *J. Hydraul. Div. Am. Soc. Civ. Eng.*, *107*, 899–918.
Hey, R. D. (1979), Flow resistance in gravel bed rivers, *J. Hydraul. Div. Am. Soc. Civ. Eng.*, *105*, 365–379.
Hey, R. D., and C. R. Thorne (1986), Stable channels with mobile gravel beds, *J. Hydraul. Eng.*, *112*, 671–689.
Higginson, N. N. J., and H. T. Johnston (1988), Estimation of friction factor in natural streams, in *Proceedings of the International Conference on River Regime*, edited by W. R. White, pp. 251–266, John Wiley, New York.
Jäggi, M. (1984), Abflussberechnung in kiesführenden Flüssen, *Wasserwirtschaft*, *74*(5), 263–267.
Jarrett, R. D. (1984), Hydraulics of high-gradient streams, *J. Hydraul. Eng.*, *110*, 1519–1539.
Kellerhals, R. (1970), Runoff routing through steep natural channels, *J. Hydraul. Div. Am. Soc. Civ. Eng.*, *96*, 2201–2217.
Keulegan, G. B. (1938), Laws of turbulent flow in open channels, *J. Res. Natl. Bur. Stand. U.S.*, *21*, 707–741.
Lamb, M. P., W. E. Dietrich, and J.-G. Venditti (2008), Is the critical Shields stress for incipient sediment motion dependent on channel-bed slope?, *J. Geophys. Res.*, *113*, F02008, doi:10.1029/2007JF000831.
Lee, A. J., and R. I. Ferguson (2002), Velocity and flow resistance in step-pool streams, *Geomorphology*, *46*, 59–71.
Lenzi, M. A. (2001), Step-pool evolution in the Rio Cordon, northeastern Italy, *Earth Surf. Processes Landforms*, *26*, 991–1008.
Lenzi, M. A., L. Mao, and F. Comiti (2004), Magnitude-frequency analysis of bed load data in an Alpine boulder bed stream, *Water Resour. Res.*, *40*, W07201, doi:10.1029/2003WR002961.
Leopold, L. B., and W. W. Emmett (1976), Bedload measurements, East Fork River, Wyoming, *Proc. Natl. Acad. Sci. U. S. A.*, *73*, 1000–1004.
Leopold, L. B., and W. W. Emmett (1977), 1976 Bedload measurements, East Fork River, Wyoming, *Proc. Natl. Acad. Sci. U. S. A.*, *73*, 2644–2648.
Leopold, L. B., and W. W. Emmett (1997), Bedload and river hydraulics—Inferences from the East Fork River, Wyoming, *U.S. Geol. Surv. Prof. Pap.*, *1583*, 52 pp.
Lepp, L. R., C. J. Koger, and J. A. Wheeler (1993), Channel erosion in steep gradient, gravel-paved streams, *Bull. Assoc. Eng. Geol.*, *4*, 443–454.
Limerinos, J. T. (1970), Determination of the Manning coefficient from measured bed roughness in natural channels, *U.S. Geol. Surv. Water Supply Pap.*, *1898-B*, 47 pp.
MacFarlane, W. A., and E. E. Wohl (2003), Influence of step composition on step geometry and flow resistance in step-pool streams of the Washington Cascades, *Water Resour. Res.*, *39*(2), 1037, doi:10.1029/2001WR001238.
Marcus, W. A., K. Roberts, L. Harvey, and G. Tackman (1992), An evaluation of methods for estimating Manning's n in small mountain streams, *Mt. Res. Dev.*, *12*, 227–239.
Meyer-Peter, E., and R. Müller (1948), Formulas for bedload transport, in Proceedings of the 2nd Meeting of the International Association of Hydraulic Structures Research, Stockholm, Sweden, pp. 39–64, Int. Assoc. Hydraul. Res., Delft, Netherlands.
Millar, R. G. (1999), Grain and form resistance in gravel-bed rivers, *J. Hydraul. Res.*, *37*, 303–312.
Millar, R. G., and M. C. Quick (1994), Flow resistance of high-gradient gravel channels, in *Hydraulic Engineering '94*, vol. 2, edited by G. V. Cotroneo and R. R. Rumer, pp. 717–721, Am. Soc. Civ. of Eng., New York.
Montgomery, R. D., and J. M. Buffington (1997), Channel-reach morphology in mountain drainage basin, *Geol. Soc. Am. Bull.*, *109*(5), 596–611.

Mussetter, R. A. (1989), Dynamics of mountain streams, Ph.D. dissertation, Colo. State Univ., Fort Collins.

Nikora, V. I., D. Goring, I. McEwan, and G. Griffiths (2001), Spatially averaged open-channel flow over rough bed, *J. Hydraul. Eng.*, *127*, 123–133.

Nikora, V. I., K. Koll, I. McEwan, D. G. McLean, and A. Dittrich (2004), Velocity distribution in the roughness layer of rough-bed flows, *J. Hydraul. Eng.*, *130*, 1036–1042.

Orlandini, S., C. Boaretti, V. Guidi, and G. Sfondrini (2006), Field determination of the spatial variation of resistance to flow along a steep Alpine stream, *Hydrol. Processes*, *20*, 3897–3913.

Palt, S. M. (2001), Sedimenttransporte im Himalaya-Karakorum und ihre Bedeutung für Wasserkraftanlagen, *Mitt. 209*, Inst. für Wasserwirtsch. und Kulturtech., Univ. Karlsruhe, Karlsruhe, Germany.

Pagliara, S., and P. Chiavaccini (2006), Flow resistance of rock chutes with protruding boulders, *J. Hydraul. Eng.*, *132*, 545–552.

Parker, G., and A. W. Peterson (1980), Bar resistance of gravel-bed streams, *J. Hydraul. Div. Am. Soc. Civ. Eng.*, *106*, 1559–1573.

Rauws, G. (1988), Laboratory experiments on resistance to overland flow due to composite roughness, *J. Hydrol.*, *103*, 37–52.

Recking, A. (2010), A comparison between flume and field bed load transport data and consequences for surface based bed load transport prediction, *Water Resour. Res.*, *46*, W03518, doi:10.1029/2009WR008007.

Recking, A., P. Frey, A. Paquier, P. Belleudy, and J. Y. Champagne (2008), Feedback between bed load and flow resistance in gravel and cobble bed rivers, *Water Resour. Res.*, *44*, W05412, doi:10.1029/2007WR006219.

Reid, D. E., and E. J. Hickin (2008), Flow resistance in steep mountain streams, *Earth Surf. Processes Landforms*, *33*, 2211–2240.

Reid, I., J. B. Laronne, and D. M. Powell (1995), The Nahal Yatir Bedload Database: Sediment dynamics in a gravel-bed ephemeral stream, *Earth Surf. Processes Landforms*, *20*, 845–857.

Rickenmann, D. (1990), Bedload transport capacity of slurry flows at steep slopes, *Mitt. 103*, 249 pp., Versuchsanst. für Wasserbau, Hydrol. und Glaziol., Eidg. Tech. Hochsch. Zürich, Zurich, Switzerland.

Rickenmann, D. (1991), Hyperconcentrated flow and sediment transport at steep slopes, *J. Hydraul. Eng.*, *117*, 1419–1439.

Rickenmann, D. (1994), An alternative equation for the mean velocity in gravel-bed rivers and mountain torrents, in *Hydraulic Engineering '94*, vol. 1, edited by G. V. Cotroneo and R. R. Rumer, pp. 672–676, Am. Soc. of Civ. Eng., New York.

Rickenmann, D. (1996), Fliessgeschwindigkeit in Wildbächen und Gebirgsflüssen, *Wasser Energie Luft*, *88*, 298–304.

Rickenmann, D. (2001), Comparison of bed load transport in torrents and gravel bed streams, *Water Resour. Res.*, *37*, 3295–3305, doi:10.1029/2001WR000319.

Rickenmann, D. (2005), Geschiebetransport bei steilen Gefällen, *Mitt. 190*, pp. 107–119, Versuchsanst. für Wasserbau, Hydrol. und Glaziol., Eidg. Tech. Hochsch. Zürich, Zurich, Switzerland.

Rickenmann, D. (2011), Alluvial steep channels: Flow resistance, bedload transport prediction and transition to debris flows, in *Gravel Bed Rivers: Processes, Tools, Environment*, edited by M. Church, P. Biron and A. Roy, John Wiley & Sons, Chichester, England.

Rickenmann, D., and A. Koschni (2010), Sediment loads due to fluvial transport and debris flows during the 2005 flood events in Switzerland, *Hydrol. Processes*, *24*, 993–1007.

Rickenmann, D., M. Chiari, and K. Friedl (2006), SETRAC—A sediment routing model for steep torrent channels, in *River Flow* 2006, edited by R. Ferreira, E. Alves, J. Leal, and A. Cardoso, pp. 843–852, Taylor and Francis, London.

Ryan, S. E., L. S. Porth, and C. A. Troendle (2002), Defining phases of bedload transport using piecewise regression, *Earth Surf. Processes Landforms*, *27*, 971–990.

Samide, G. W. (1971), Sediment transport measurements, Ph.D. dissertation, Univ. of Alberta, Edmonton, Alberta, Canada.

Smart, G. M., and M. N. R. Jäggi (1983), Sediment transport on steep slopes, *Mitt. 64*, pp. 89–191, Versuchsanst. für Wasserbau, Hydrol. und Glaziol., Eidg. Tech. Hochsch. Zürich, Zurich, Switzerland.

Strickler, K. (1923), Beiträge zur Frage der Geschwindigkeitsformel und der Rauhigkeitszahlen für Ströme, Kanäle und geschlossene Leitungen, *Mitt. 16*, Eidg. Amt für Wasserwirtsch., Bern, Switzerland.

Thorne, C. R., and L. W. Zevenbergen (1985), Estimating mean velocity in mountain rivers, *J. Hydraul. Eng.*, *111*, 612–624.

Tsujimoto, T. (1991), Bed-load transport in steep channels, in *Fluvial Hydraulics of Mountain Regions, Lect. Notes Earth Sci. Ser.*, vol. 37, pp. 89–102, Springer, Berlin.

Turowski, J. M., E. M. Yager, A. Badoux, D. Rickenmann, and P. Molnar (2009), The impact of exceptional events on erosion, bedload transport and channel stability in a step-pool channel, *Earth Surf. Processes Landforms*, *34*, 1661–1673.

Wang, J., Z. Dong, C. Chen, and Z. Xia (1993), The effects of bed roughness on the distribution of turbulent intensities in open channel flow, *J. Hydraul. Res.*, *31*, 89–98.

Wargadalam, J. (1993), Hydraulic geometry equations of alluvial channels, 203 pp., Ph.D. dissertation, Colo. State Univ., Fort Collins.

Wiberg, P., and J. D. Smith (1991), Velocity distribution and bed roughness in high-gradient streams, *Water Resour. Res.*, *27*, 825–838, doi:10.1029/90WR02770.

Wilcox, A., J. M. Nelson, and E. E. Wohl (2006), Flow resistance dynamics in step-pool channels: 2. Partitioning between grain, spill, and woody debris resistance, *Water Resour. Res.*, *42*, W05419, doi:10.1029/2005WR004278.

Williams, G. P., and D. L. Rosgen (1989), Measured total sediment loads (suspended loads and bedloads) for 93 United States streams, *U.S. Geol. Surv. Open File Rep.*, *89–67*, 128 pp.

Wohl, E., and A. Wilcox (2005), Channel geometry of mountain streams in New Zealand, *J. Hydrol.*, *300*, 252–266.

Wong, M., and G. Parker (2006), Reanalysis and correction of bed-load relation of Meyer-Peter and Müller using their own database, *J. Hydraul. Eng.*, *132*, 1159–1168.

Yager, E. M., J. W. Kirchner, and W. E. Dietrich (2007), Calculating bed load transport in steep boulder bed channels, *Water Resour. Res.*, *43*, W07418, doi:10.1029/2006WR005432.

Yen, B. C. (2002), Open channel flow resistance, *J. Hydraul. Eng.*, *128*, 20–38.

Zimmermann, A. (2010), Flow resistance in steep streams: An experimental study, *Water Resour. Res.*, *46*, W09536, doi:10.1029/2009WR007913.

A. Recking, UR Erosion Torrentielle Neige Avalanches, Cemagref, 2 rue de la papeterie, BP 76, F-38402 Saint-Martin-d'Hères, France. (alain.recking@cemagref.fr)

D. Rickenmann, Swiss Federal Research Institute WSL, CH-8903 Birmensdorf, Switzerland. (rickenmann@wsl.ch)